Combinatorics of bicubic maps with hard particles

2005 J. Phys. A: Math. Gen. 38 4529

(http://iopscience.iop.org/0305-4470/38/21/002)

INSTITUTE OF PHYSICS PUBLISHING JOURNAL OF PHYSICS A: MATHEMATICAL AND GENERAL

J. Phys. A: Math. Gen. **38** (2005) 4529–4559 doi:10.1088/0305-4470/38/21/002

Combinatorics of bicubic maps with hard particles

J Bouttier[1,2], **P Di Francesco**[1] **and E Guitter**[1]

[1] Service de Physique Théorique, CEA/DSM/SPhT, Unité de recherche associée au CNRS, CEA/Saclay, 91191 Gif sur Yvette Cedex, France
[2] Instituut voor Theoretische Fysica, Valckeniertstraat 65, 1018 XE Amsterdam, The Netherlands

E-mail: bouttier@spht.saclay.cea.fr, philippe@spht.saclay.cea.fr and guitter@spht.saclay.cea.fr

Received 24 January 2005, in final form 24 March 2005
Published 10 May 2005
Online at stacks.iop.org/JPhysA/38/4529

Abstract

We present a purely combinatorial solution of the problem of enumerating planar bicubic maps with hard particles. This is done by the use of a bijection with a particular class of blossom trees with particles, obtained by an appropriate cutting of the maps. Although these trees have no simple local characterization, we prove that their enumeration may be performed upon introducing a larger class of 'admissible' trees with possibly doubly occupied edges and summing them with appropriate signed weights. The proof relies on an extension of the cutting procedure allowing for the presence on the maps of special non-sectile edges. The admissible trees are characterized by simple local rules, allowing eventually for an exact enumeration of planar bicubic maps with hard particles. We also discuss generalizations for maps with particles subject to more general exclusion rules and show how to re-derive the enumeration of quartic maps with Ising spins in the present framework of admissible trees. We finally comment on a possible interpretation in terms of branching processes.

PACS numbers: 05.50.+q, 04.60.Nc, 61.50.Ks, 64.60.−i

1. Introduction

Enumeration of planar maps has been a constant subject of interest for both mathematicians and physicists. Many exact enumeration formulae have been obtained over the years for various types of maps, say maps with fixed vertex and/or face valences, maps with particular colour prescriptions, or even maps carrying additional degrees of freedom such as spins or particles. Since the original combinatorial approach of Tutte [1], two general methods of enumeration have been developed. The first one uses *matrix integrals* [2, 3] of the form $\int \exp[-N\mathrm{Tr}U]$ over possibly several $N \times N$ Hermitian matrices and with an action U designed so that the diagrammatic expansion precisely reproduces the maps to be enumerated. For a large class

of maps, a direct computation of the associated matrix integral may be carried out exactly, thus providing explicit enumeration formulae. These calculations rely on various techniques: saddle point methods [2], orthogonal polynomial methods [4], as well as the so-called loop equation method [5, 6], very similar in spirit to Tutte's original work. Beyond matrix integrals, another, more recently developed technique relies on the existence of *bijections* between planar maps and decorated trees, reducing the problem to that, much simpler, of counting trees [7–15]. In most cases, the trees at hand are easily constructed recursively and recursion formulae may therefore be derived for the generating functions of the maps. The main interest of this technique is clearly its conceptual simplicity, as it uses only elementary combinatorics. Another advantage is that it also gives access to refined properties of the maps. For instance, the statistics of distances between points on the maps, already addressed in [16–19] by a specific combinatorial treatment, emerges naturally from the bijective formalism [20–24].

The matrix integral and bijective techniques above are *a priori* very different in nature but, remarkably enough, in all cases which have been solved by both methods, the precise form of the solution involves very similar systems of algebraic equations. That algebraic equations appear as recursive equations for generating functions of trees should not come as a surprise. What is more surprising is that the matrix integral solution comes precisely in the *same* form, allowing us to interpret the somewhat abstract auxiliary functions of this matrix integral solution as generating functions for trees. Even if we have no direct understanding of this phenomenon, this simple observation allows us to use the matrix integral solution for a particular map enumeration problem as a tool to *guess* how to characterize the ensemble of trees in bijection with these maps. This already proved very useful for various classes of maps and this paper will show another example where applying such a principle leads to the combinatorial, bijective solution of a quite involved problem, namely the combinatorics of bicubic maps with hard particles.

Before we proceed to our study, let us recall more precisely to which families of maps the methods above have been applied so far. We may classify the problems in the matrix integral language according to the number of (Hermitian) matrices needed to reproduce the desired maps. The simplest case of the so-called one-matrix integral over a matrix M with action

$$U(M) = \frac{M^2}{2} - \sum_{k\geqslant 1} g_k \frac{M^k}{k} \tag{1.1}$$

corresponds to maps with prescribed weights g_k per k-valent vertex and was solved extensively in [2]. Its tree formulation involves the so-called *blossom trees* [9] with 'charged' decorations, and with simple charge characterizations [13]. The next case is that of the so-called two-matrix model involving an integral over two matrices B and W interacting only via a term BW, namely with action

$$U(B, W) = BW - \sum_{k\geqslant 1} g_k \frac{B^k}{k} - \sum_{k\geqslant 1} \tilde{g}_k \frac{W^k}{k}. \tag{1.2}$$

This model corresponds to having *bipartite* maps, i.e. maps with two types of vertices, say black and white, such that all edges connect vertices of opposite colours, and with prescribed weights g_k, $\tilde{g}_k$ according to the valence *and* the colour of the vertices. This matrix model was also solved extensively [25]. Its tree version involves again blossom trees with now slightly more involved charge characterizations [14, 15]. Note that the one-matrix model may be viewed as a particular case of the two-matrix model with $g_k = \delta_{k,2}$, in which case the matrix B may be formally integrated out. In the map language, this simply states that arbitrary maps are in bijection with bipartite maps whose black vertices all have valence 2, as is clear by inserting a bivalent black vertex in the middle of each edge. More generally, we

may always decide to suppress all (black or white) bivalent vertices of a bipartite map, thus creating maps whose black and white vertices may be connected regardless of their colour, and which now carry edge weights depending on the relative colours of their adjacent vertices. The two-matrix model or its equivalent tree formulation gives for instance access to maps carrying configurations of the Ising model [14] or maps with hard particles [15].

This exhausts the classes of maps which could be enumerated both via matrix integrals and bijective methods. On the other hand, it is well known that multi-matrix integrals over, say, m matrices $M_1, \ldots, M_m$ and with *chain interaction*, namely

$$U(M_1, \ldots, M_m) = \sum_{i=1}^{m-1} c_i M_i M_{i+1} - \sum_{i=1}^{m} \sum_{k \geqslant 1} g_k^{(i)} \frac{M_i^k}{k} \tag{1.3}$$

are completely calculable by means of bi-orthogonal polynomial techniques and give rise to solutions expressible in terms of abstract auxiliary functions solutions of algebraic equations [3]. These turn out to describe quite generally maps with particles subject to some *exclusion rules*. More precisely, the above m-matrix model describes maps with particles occupying the vertices and with the edge exclusion constraint that the *total* number of particles at the ends of any edge does not exceed $m - 1$. In the case of even $m = 2p$, the model alternatively describes bipartite maps with particles such that the total number of particles at the ends of any edge now does not exceed[3] $p - 1$. For all these models, the algebraic nature of the solution suggests that again a bijection with trees should exist.

The aim of this paper is precisely to extend the bijective techniques to maps with particles subject to edge exclusion rules. Very generally, the physical motivation for considering such models is to construct simple solvable models describing gases of interacting particles. This was first achieved on regular two-dimensional lattices with the so-called *hard-core lattice gas*, providing the simplest possible model of a dense fluid which incorporates the excluded volume effect [26]. An exact solution for this model was obtained by Baxter in [27], in the case of hard particles living on the vertices of the triangular lattice (the so-called hard hexagon model). It displays a crystallization transition from a low density disordered phase to a high density ordered (crystalline) phase in which particles tend to occupy preferentially one of the three canonical sublattices of the (tripartite) triangular lattice. The transition was identified to be in the universality class of the critical 3-state Potts model, in agreement with the 3-fold symmetry of the crystalline groundstates. The square and hexagonal lattice versions of the hard-core lattice gas, corresponding respectively to hard squares and hard triangles, could not be solved exactly. Still, numerical evidence points to a crystallization transition now in the class of the critical Ising model [28], consistent with the twofold symmetry of the groundstates, in which particles occupy one of the two canonical sublattices of these bipartite lattices. This hunt for exact solutions led to consider the hard-core gas model on random lattices, in the form of planar maps with hard particles. It was recognized in [29] that the crystallization transition is wiped out for the statistical ensemble of arbitrary maps but that it is restored when restricting the class of maps to bipartite ones. Simple examples are hard particles on planar bicubic or biquartic maps, which may be seen as the randomized, bipartite versions of the hard triangle and hard square models. These were solved exactly in [29] and shown to display a crystallization transition in the class of the critical Ising model on random graphs. Indeed, the bipartite nature of the maps grants the existence of two crystalline maximally occupied groundstates, with particles lying on one of the two canonical subgraphs of the

[3] The equivalence between the two formulations is obtained as follows: starting from the bipartite formulation with the edge rule of at most $p-1$ particle occupancy, we single out bivalent black-empty vertices and erase them, resulting in an effective modified edge rule that amounts to having at most $2p-1$ particles per edge upon reinterpreting black ℓ-occupied vertices as white $(p+\ell)$-occupied ones.

maps. More generally, the above models of particles on bipartite maps with the exclusion rule of at most $p-1$ particles per edge allow us to attain multi-critical transition points. When $p=3$ for instance, a tricritical point in the class of the tricritical Ising model may be reached [29], separating a line of Ising-like transition points from a line of first-order transition points between groundstates of different symmetry.

In this paper, we concentrate mainly on *planar bicubic maps with hard particles*, i.e. bipartite maps with black and white trivalent vertices and the exclusion rule that each edge has at most one adjacent particle. In the graph theory language, planar bicubic maps correspond to planar bipartite 3-regular (multi-)graphs and a configuration of hard particles in such a map corresponds to an independent or stable set in the graph. In the matrix language, this model is described by a four-matrix integral with action

$$U(M_1,\dots,M_4) = M_1M_2 - M_2M_3 + M_3M_4 - g\left(\frac{M_1^3}{3}+\frac{M_4^3}{3}\right) - gz\left(\frac{M_2^3}{3}+\frac{M_3^3}{3}\right) \qquad (1.4)$$

where g is a weight per vertex and z is a weight per particle. The explicit algebraic solution of this matrix integral was given in [29]. In this paper, we show how to re-derive this solution in a purely combinatorial way using bijections with suitable classes of blossom trees with particles. As opposed to bipartite maps without particles (two-matrix model), a new feature of this construction is that we have to resort to a kind of inclusion–exclusion principle in which doubly occupied edges are *a priori* allowed but are effectively subtracted by appropriate sign factors.

The paper is organized as follows. In section 2, we recall the definition of bicubic maps with hard particles and present the matrix model results of [29], as well as the underlying physics. Section 3 presents our main theorem, namely the existence of a blossom tree formulation of the model in terms of the so-called 'admissible trees' whose enumeration with appropriate signed weights reproduce that of planar bicubic maps with hard particles. The definition of blossom trees without particles is recalled in section 3.1. We then define in section 3.2 admissible trees as blossom trees with particles and with specific charge characterizations and state our main theorem relating the generating function of bicubic maps with particles to that of admissible trees with signed weights. The characterization of admissible trees is used to list all their possible local environments (section 3.3) and to derive a system of algebraic equations which determines their desired signed generating function (section 3.4), reproducing the results of [29]. The proof of the map/tree equivalence is given in sections 4 and 5. It is based on a general cutting procedure of bicubic maps into trees (section 4.1) adapted so as to allow for 'special' *non-sectile* edges on the map (section 4.2). This generalized cutting procedure is used in section 4.3 to construct a bijection between trees and maps, both with special edges. It is used in section 5.1 in the case of bicubic maps with hard particles to organize admissible trees into equivalence classes represented by 'admissible maps', of which bicubic maps with hard particles are only a subset. The characterization of these equivalence classes (section 5.2) allows us to show that, in the enumeration of admissible trees with appropriate signed weights, the contribution of an equivalence class is zero unless the admissible map satisfies the hard-particle constraint (section 5.3). This proves that the generating function for signed admissible trees matches that of bicubic maps with hard particles. Finally, we discuss in section 6 various generalizations of this map/tree equivalence for the Ising model on quartic maps (section 6.1) or maps with generalized edge exclusion rules (section 6.2). We also discuss a corollary of our construction, namely the existence of an Ising-like crystallization transition for a statistical ensemble of trees with particles and comment on a possible branching process interpretation. We gather a few concluding remarks in section 7.

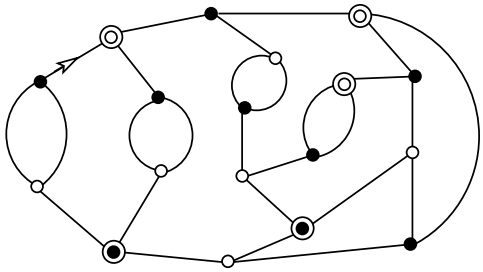

Figure 1. An example of bicubic map with hard-particles. The vertices are of four types: black-empty, white-empty, black-occupied and white-occupied, represented respectively by $\bullet$, $\circ$, $\odot$ and $\circledcirc$. All vertices have valence three and adjacent vertices have different colours. The hard-particle constraint states that no two adjacent vertices are simultaneously occupied. The map is rooted at the edge indicated by the arrow, originating from a black-empty vertex and with the external face on its left.

2. The problem of bicubic maps with hard particles and its matrix integral solution

2.1. Hard particles on bicubic maps

As mentioned in the introduction, we will mainly study in this paper *bicubic maps with hard particles*, namely planar maps with black and white trivalent vertices and edges connecting only vertices of opposite colour. The vertices may be occupied or not by particles, with the *hard-particle constraint* such that no edge has two adjacent occupied vertices. The map is assumed to contain at least one black-empty vertex and it is furthermore rooted, i.e. carries a marked oriented edge pointing from one of its black-empty vertices (the root vertex). An example of such a map is depicted in figure 1. In the planar representation, we always chose for external face that on the left of the root edge. We are interested in enumerating these maps with, say $n_\circ$ white-empty, $n_\bullet + 1$ black-empty, $n_{\circledcirc}$ white-occupied and $n_\odot$ black-occupied vertices. For simplicity, we will concentrate here on the slightly easier task of computing the *generating function* $G_{\rm BMHP}(g, z)$ for these maps with, say a weight g per empty or occupied, black or white vertex, and a weight z per particle, namely

$$G_{\rm BMHP}(g, z) = \sum_{m,n} g^n z^m \mathcal{B}_{n,m} \tag{2.1}$$

where $\mathcal{B}_{n,m}$ denotes the total number of planar bicubic maps rooted at a black-empty vertex with a total number $n = n_\circ + n_\bullet + n_{\circledcirc} + n_\odot + 1$ of vertices and a total number $m = n_{\circledcirc} + n_\odot$ of particles.

2.2. Matrix integral solution

The generating function $G_{\rm BMHP}(g, z)$ was obtained in [29] by use of a four-matrix integral with action (1.4). The result involves four auxiliary functions R, S, T and V depending on g and z and solution of a closed algebraic system:

$$\begin{aligned} S &= 1 + 2gR & T &= -g^3 z V^4 \\ R &= gV^2 + gzS^2 + 2g^2 zT & V &= S + 2g^2 zVS \end{aligned} \tag{2.2}$$

which determines them uniquely order by order in g provided we take $V = 1 + \mathcal{O}(g)$. The planar free energy $F_{\rm BMHP}(g, z)$ of the model, counting *unrooted* bicubic maps with hard

particles, and without the constraint of having at least one black-empty vertex, is related to these functions via

$$\left(\frac{1}{g}\frac{\mathrm{d}}{\mathrm{d}g}\right)^2 g^4 F_{\mathrm{BMHP}}(g,z) = 4\,\mathrm{Log}\,V(g,z). \tag{2.3}$$

The generating function $G_{\mathrm{BMHP}}(g,z)$ is related to the free energy via

$$G_{\mathrm{BMHP}}(g,z) = \frac{3}{2}\left(g\frac{\mathrm{d}}{\mathrm{d}g} - z\frac{\mathrm{d}}{\mathrm{d}z}\right) F_{\mathrm{BMHP}}(g,z) \tag{2.4}$$

where the derivatives amount to marking a vertex ($g\,\mathrm{d}/\mathrm{d}g$) which is not occupied ($-z\,\mathrm{d}/\mathrm{d}z$). The prefactor $1/2$ amounts to assuming that this vertex is black and the factor 3 stands for the three choices of an adjacent rooted edge. Strictly speaking, we must use the black–white symmetry of the maps counted by F_{BMHP} which imposes that there are in average as many black-empty vertices as white-empty ones.

A straightforward, though tedious exercise allows by a Lagrange inversion to get a closed formula for the coefficient G_{2n} of g^{2n} in $G_{\mathrm{BMHP}}(g,z)$ (note that G_{BMHP} has only even powers of g as bicubic maps always have an equal number of black and white vertices). Details can be found in [30], with the result

$$G_{2n}(z) = \frac{3}{2}\frac{2^n}{(n+1)(n+2)} \sum_{0\leqslant 2p\leqslant j\leqslant n} \left(-\frac{1}{2}\right)^p \binom{2n-j}{n}\binom{n-j}{p}\binom{4n-2j}{j-2p} z^j. \tag{2.5}$$

2.3. Phase diagram

A nice outcome of the above algebraic solution is the existence of a critical line $g_c(z)$ governing the large n growth of G_{2n}, namely

$$G_{2n} \sim \frac{g_c(z)^{-2n}}{n^{5/2}} \tag{2.6}$$

for generic values of z. The value of $g_c(z)$ is easily obtained from the singularity of G_{BMHP} with the result

$$g_c^2(z) = \begin{cases} \dfrac{1}{8z} - \dfrac{1}{4z^2} & \text{for} \quad z \geqslant z_+ \\ \dfrac{1+8u+10u^2}{8(1+2u)^8} \quad \text{if} \quad z = 4u(1+2u)^4 & \text{for} \quad z_- \leqslant z \leqslant z_+. \end{cases} \tag{2.7}$$

Physically, the quantity $\mathrm{Log}\,g_c(z)$ may be interpreted as a free energy per vertex. As explained in [29], the two values z_- and z_+ correspond to two special points

$$\begin{aligned} g_- &= \frac{5^3\sqrt{15}}{2^{10}}, \qquad & z_- &= -\frac{2^9}{5^5} \\ g_+ &= \frac{\sqrt{15}}{2^6}, & z_+ &= 2^5 \end{aligned} \tag{2.8}$$

at which the model becomes 'tricritical' with a large n behaviour

$$G_{2n} \sim \frac{g_\pm^{-2n}}{n^{7/3}}. \tag{2.9}$$

The first tricritical point (g_-) occurs at a (rather unphysical) negative value of z and corresponds to the so-called Lee–Yang edge singularity. The second tricritical point (g_+) occurs at a positive value of z and corresponds to a change of determination of $g_c(z)$ in equation (2.7), i.e. of the

free energy. Physically, it corresponds to a *crystallization transition* point above which particles tend to lie preferentially on vertices of a given colour. This may be seen by breaking the symmetry between black and white vertices upon introducing different weights $z_\circ$ and $z_\bullet = z^2/z_\circ$ for particles occupying white or black vertices and by computing the difference of the densities of particles on the black and the white sublattice. Letting $z_\circ \to z$ from the above yields a non-zero density difference for $z > z_+$ while the density difference vanishes for $z \leqslant z_+$. This transition lies in the universality class of the Ising model on random lattices. This is corroborated by computing from equation (2.7) the order of the discontinuity of the free energy at z_+: one finds a discontinuity in the third derivative, immediately translated into a 'thermal exponent' $\alpha = -1$, identified with that of the Ising transition on random graphs [31].

3. Combinatorics of bicubic maps with hard particles via blossom trees: main results

The aim of this paper is to provide an alternative derivation of the set of equations (2.2) above by a purely combinatorial approach based on the cutting of maps into the so-called 'blossom trees'. This approach is similar in spirit to the bijective methods developed in [9] using one-to-one correspondences between, on the one hand, various classes of rooted planar maps and, on the other hand, blossom trees, i.e. trees with appropriate 'charged' decorations (the so-called buds and leaves) and simple charge characterizations. In the present case, a similar bijection also exists between rooted bicubic maps with hard particles and a particular class of blossom trees, which we shall refer to as *good* trees. These good trees, however, have no simple charge characterization and, as such, do not allow for a simple enumeration. Fortunately, we may rely on a more general many-to-one correspondence between what we shall call *admissible* trees, now with an easy charge characterization, and a larger class of bicubic maps with particles. The generating function for the admissible trees with appropriate signed weights turns out to match exactly that of good trees, and therefore enumerates the desired rooted bicubic maps with hard particles. This is the key for our combinatorial approach.

3.1. Blossom trees

The combinatorial enumeration of planar bicubic maps *without particles* involves a bijection with the so-called *blossom trees*. A blossom tree is a plane tree satisfying the following properties:

(1) Its inner vertices are of two types: black or white, all of valence three.
(2) It is bicoloured, i.e. all its inner edges connect only black inner vertices to white ones.
(3) It has two kinds of leaves: the so-called *buds*, connected only to black inner vertices and the so-called *leaves*, connected only to white inner vertices. We attach a *charge* -1 to each bud and a charge +1 to each leaf.
(4) Its total charge (no. of leaves $-$ no. of buds) is equal to 3.

Note that this last property is equivalent to imposing that there is exactly one more white vertex than black ones in the tree. Moreover, a direct consequence of the defining properties (1)–(4) is that each inner edge of a blossom tree separates it into a piece of total charge $q_\circ \equiv 2 \bmod 3$ starting with a white vertex, and a piece of total charge $q_\bullet = 3 - q_\circ \equiv 1 \bmod 3$ starting with a black vertex. Such an edge will be called of type $(q_\circ : q_\bullet)$.

A blossom tree may be closed into a map as follows: we consider the anti-clockwise sequence of buds and leaves around the tree and decide to connect all pairs made of a bud

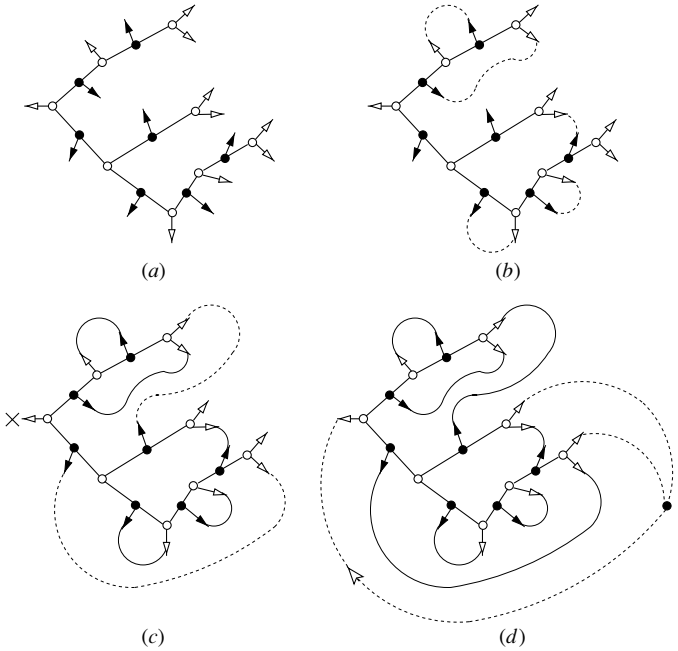

Figure 2. An example of blossom tree (*a*). Here and throughout the paper, buds are represented by black arrows and leaves by white arrows. The tree may be closed into a bicubic map (*d*) as follows: each pair of anti-clockwise consecutive bud–leaf is glued into an edge (*b*). The process is repeated (*c*) until one is left with exactly three unmatched leaves. The latter are connected (*d*) to an additional black vertex, thus producing a planar bicubic map. Choosing one of the three unmatched leaves as a root for the blossom tree (crossed in (*c*)) amounts to rooting the map (white arrow in (*d*)).

immediately followed by a leaf so as to form an edge (see figure 2). Iterating this procedure, we end up with exactly three *unmatched* leaves, as the total charge of the tree is 3. These unmatched leaves are then connected to an additional black vertex in the external face. The net result is clearly a planar bicubic map. In the following, we will make use of *rooted* blossom trees, i.e. trees with a distinguished leaf serving as root. More precisely, we shall always pick the root among the three unmatched leaves of the tree. Via the above closing procedure, this allows us to generate a rooted bicubic map, i.e. a map with a marked oriented edge, namely that pointing from the additional black vertex to the chosen unmatched leaf.

Conversely, any bicubic map may be cut into a blossom tree. The precise cutting procedure will be recalled in section 4.1 below. The blossom trees thus obtained form a restricted class, subject to specific restrictions which ensure that the charge is evenly distributed along the tree. More precisely, an edge of type $(q_\circ : q_\bullet)$ is said to be *regular* if and only if it satisfies $q_\circ \geqslant 0$ and $q_\bullet \leqslant 1$. Any edge that is not regular is called *non-regular*. The trees obtained by cutting bicubic maps satisfy the additional constraint that all their inner edges are regular[4]. This furthermore leads to a bijection between rooted planar bicubic maps and blossom trees with only regular inner edges, rooted at one of their three unmatched leaves [11, 12]. In this framework, the cutting/closing procedures are moreover inverse of one another.

[4] For the blossom trees at hand, this property simply amounts to imposing that there is exactly one bud attached to each black vertex. The tree of figure 2(*a*) satisfies this property.

3.2. Admissible trees and main theorem

We would like to extend the above bijection to the case of bicubic maps with hard particles. A natural candidate for the trees to be considered are blossom trees satisfying (1)–(4) above, with all their inner edges regular, and now carrying particles satisfying the hard-particle constraint. In the following, we shall denote by *HP* any edge that satisfies the hard-particle constraint and *NHP* (non-hard-particle) any doubly occupied edge. In other words, it seems natural to introduce 'HP-regular' blossom trees, i.e. blossom trees with particles whose inner edges are both HP and regular. Clearly, the standard cutting procedure of bicubic maps, performed regardless of particles, will produce such trees. Unfortunately, not all the HP-regular blossom trees are created that way. Indeed for an arbitrary HP-regular tree, the closing procedure may produce a map with NHP edges if two occupied vertices get connected in the process. If so, the tree at hand does not arise from the cutting of bicubic maps with particles. We may still define *good* trees as the blossom trees whose inner edges are all HP and regular and whose closing does not create NHP edges. The (rooted) good trees are in bijection with (rooted) planar bicubic maps with hard particles. However, these trees have no simple local characterization and cannot serve as such to enumerate the maps.

This is the reason why we are led to consider a larger class of blossom trees, which we shall call *admissible*. As opposed to good trees, the hard-particle condition need not be fulfilled on admissible trees and edges may be NHP on the tree. The key point will be, however, to correlate the NHP character of inner edges to their non-regularity. More precisely, we define an admissible tree as a blossom tree satisfying properties (1)–(4), further completed by the condition that each inner vertex may be occupied or not by a particle, and with the two extra conditions:

(5) All HP edges of the tree are regular.
(6) All NHP edges of the tree are non-regular.

Thanks to properties (1)–(4), these two conditions may be rephrased into

(5′) Every HP edge is of type $(q_\circ : q_\bullet)$ with $q_\circ \geqslant 2$, hence $q_\bullet \leqslant 1$.
(6′) Every NHP edge is of type $(q_\circ : q_\bullet)$ with $q_\circ \leqslant -1$, hence $q_\bullet \geqslant 4$.

Examples of admissible and non-admissible blossom trees are displayed in figure 3. As before, we will make use of rooted admissible trees, i.e. admissible trees with a distinguished leaf among their three unmatched ones (marked by a cross on the examples of figure 3).

In the absence of NHP edges, requirement (5) states that all edges are regular. The good trees are therefore a particular subclass of the admissible trees. As it turns out, the former may be obtained from the latter via an inclusion–exclusion principle which allows us to enumerate the good trees by counting admissible trees with appropriate signed weights. This is our main result, stated as follows.

Main theorem. For any admissible tree $\mathcal{T}$, we denote by $n(\mathcal{T})$ the number of its NHP edges. We have the following sum rule:

$$\sum_{\substack{\text{rooted admissible}\\ \text{trees } \mathcal{T}}} (-1)^{n(\mathcal{T})} = \sum_{\substack{\text{rooted bicubic maps}\\ \text{with particles } \mathcal{M}}} 1 = \sum_{\substack{\text{rooted good}\\ \text{trees } \mathcal{T}}} 1. \tag{3.1}$$

Here the first and last sums run over all (admissible, resp. good) trees with fixed numbers $n_\bullet, n_\circ, n_{\odot}$ and $n_{\circledcirc}$ of black-empty, white-empty, black-occupied and white-occupied vertices. These trees are rooted at one of their three unmatched leaves. The middle sum runs over planar maps with the same numbers $n_\circ, n_{\odot}$ and $n_{\circledcirc}$ of white-empty, black-occupied and white-occupied vertices and with $n_\bullet + 1$ black-empty vertices. These maps are rooted maps, with a marked oriented edge originating from one of these $n_\bullet + 1$ black-empty vertices.

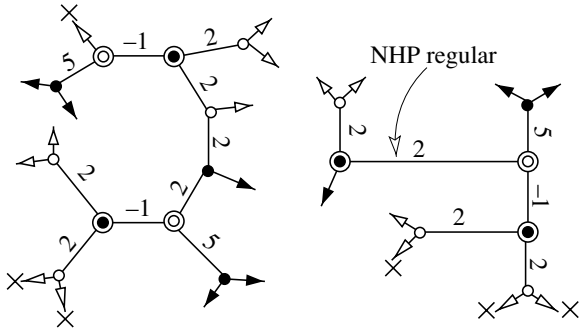

(*a*) admissible (*b*) non−admissible

Figure 3. An example of (*a*) admissible and (*b*) non-admissible blossom tree. As in figure 1, black-empty, white-empty, black-occupied and white-occupied inner vertices are represented respectively by $\bullet$, $\circ$, $\circledcirc$ and $\circledcirc$. For both trees (*a*) and (*b*), the total charge is 3 hence there are exactly three unmatched leaves, here marked by a cross. For each inner edge, we have indicated the value $q_\circ$ of the total charge for the part of the tree lying on the side of its white (empty or occupied) adjacent vertex (the reader may immediately recover the value of $q_\bullet = 3 - q_\circ$). All edges satisfy $q_\circ \equiv 2 \bmod 3$. An edge is regular when $q_\circ \geqslant 2$. In (*a*), all HP edges are regular and all NHP edges are non-regular, hence the tree is admissible. This is not the case in (*b*) where the indicated edge is both regular and NHP.

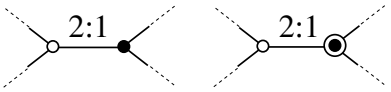

Figure 4. Inner edges adjacent to a white-empty vertex are HP, regular of type ($q_\circ = 2 : q_\bullet = 1$), and connect it to a black-empty or -occupied vertex.

As the admissible trees have a simple charge characterization, their enumeration, with the appropriate signed weight, is easily performed via a recursive construction. The above sum rule allows us to directly re-interpret this enumeration as counting rooted bicubic maps with hard particles.

3.3. Local environments

In order to enumerate admissible trees, it proves useful to first inspect all possible environments of an edge or a vertex on the tree and to characterize them in terms of charges. The above characterizations (1)–(6) of admissible trees strongly limit these possible charge environments. A first limitation concerns the local environment of white-empty vertices. Indeed, any such vertex is adjacent to either leaves, with charge +1, or inner HP edges, which are thus regular with $q_\bullet \leqslant 1$. As the vertex is trivalent and the total charge of the tree is 3, we immediately deduce that only $q_\bullet = 1$ is possible. Any inner edge attached to a white-empty vertex is therefore of type ($q_\circ = 2 : q_\bullet = 1$) (see figure 4).

Let us now consider the environment of a NHP inner edge e connecting a black-occupied vertex v to a white-occupied vertex w (see figure 5). From (6'), the charge $q_\bullet$ of the piece of the tree attached to v satisfies $q_\bullet \geqslant 4$. This piece is made of two parts, each attached to v by one of its two remaining adjacent edges (other than e). As their respective charges add up to $q_\bullet \geqslant 4$, at least one of these two parts must carry a charge greater or equal to 2, hence the corresponding edge adjacent to v must be a regular inner edge. This edge connects v to a white vertex, and, as it is regular, it must be HP, hence this white vertex is empty. We

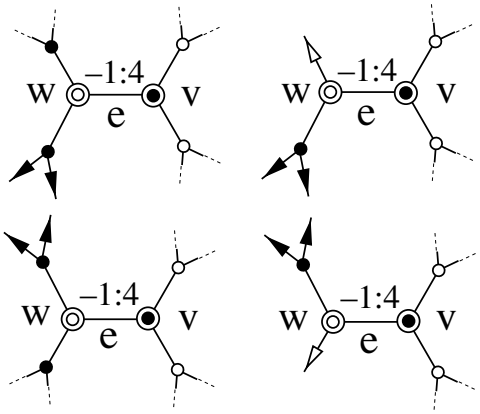

Figure 5. The four possible environments around a NHP edge. The NHP edge is necessarily of type ($q_\circ = -1 : q_\bullet = 4$). All other inner edges are HP regular of type ($q_\circ = 2 : q_\bullet = 1$) except for the edge connecting w to the black-empty vertex with two buds, which is HP regular of type ($q_\circ = 5 : q_\bullet = -2$).

deduce from the above characterization around white-empty vertices that the charge of this part is exactly 2. The charge $q_\bullet - 2$ of the other part is thus greater or equal to 2 and from the same argument, it must be 2 as well, starting from a regular inner edge connecting v to a white-empty vertex. We finally deduce that $q_\bullet = 4$, hence a complementary charge $q_\circ = -1$ for the piece of the tree starting from the white-occupied vertex w. This piece is also made of two parts, each attached to w by one of the two remaining adjacent edges (other than e). One of these parts must carry a charge less than $-1/2$, hence it must be a regular edge connecting w to a black-empty vertex. As all inner edges originating from a black-empty vertex are HP, thus regular with an attached charge larger than 2, the only way to have a charge less than $-1/2$ is that this black-empty vertex be connected to two buds, with a total charge of -2. The second part attached to w therefore has charge 1, hence is either a leaf or a regular inner edge connecting w to a black-empty vertex. To conclude, we find that all NHP edges are of type ($q_\circ = -1 : q_\bullet = 4$) with one of the four environments displayed in figure 5.

If we finally consider HP, thus regular inner edges, we already know from the above analysis around white-empty vertices that these edges are of type ($q_\circ = 2 : q_\bullet = 1$) when the adjacent white vertex is empty, irrespective of the empty or occupied state of the adjacent black vertex (see figure 4). It remains to consider the case of an inner edge connecting a black-empty to a white-occupied vertex. Such an edge is clearly either of type ($q_\circ = 2 : q_\bullet = 1$), or of type ($q_\circ = 5 : q_\bullet = -2$). In this latter case, the black-empty vertex is necessarily attached to two buds, while the white-occupied vertex is necessarily adjacent to exactly one NHP edge (see figure 6). This exhausts all possible inner edge environments.

The vertex environments follow directly from these inner edge environments, plus the possibility of attaching a leaf to white-empty or -occupied vertices and a bud to black-empty or -occupied vertices. The vertex environments are moreover subject to the constraint of total charge 3 of the tree.

3.4. Recursive equations

We are now ready for a combinatorial enumeration of admissible trees. More precisely, we want to compute the generating function $G(g, z)$ for admissible trees rooted at one of their

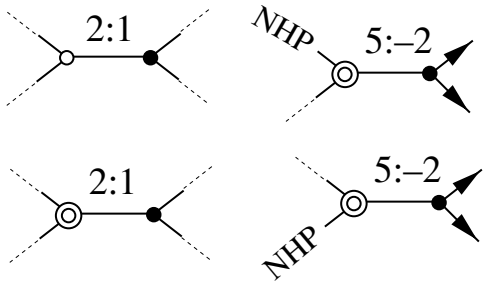

Figure 6. Inner edges adjacent to a black-empty vertex are HP, regular of type ($q_\circ = 2 : q_\bullet = 1$) or ($q_\circ = 5 : q_\bullet = -2$). In this latter case the black-empty vertex is connected to two buds and the white vertex is occupied and adjacent to exactly one NHP edge.

three unmatched leaves, with weights g per vertex and z per particle (i.e. a total weight of gz per occupied vertex) and with *a weight* -1 *per NHP inner edge* so as to reproduce the generating function for good trees according to equation (3.1).

This enumeration is simplified by considering *planted* trees, i.e trees with a distinguished leaf or bud. As all leaves except for the three unmatched ones are paired with buds, we may write

$$G(g, z) = G_{\text{leaf}}(g, z) - G_{\text{bud}}(g, z) \tag{3.2}$$

in terms of the generating functions $G_{\text{leaf}}(g, z)$ (resp. $G_{\text{bud}}(g, z)$) of admissible trees with a distinguished leaf (resp. bud). From the main theorem (3.1), this equation translates into

$$G_{\text{BMHP}}(g, z) = g(G_{\text{leaf}}(g, z) - G_{\text{bud}}(g, z)) \tag{3.3}$$

where $G_{\text{BMHP}}(g, z)$ is as before the generating function for planar bicubic maps with hard particles, with a marked oriented edge originating from a black-empty vertex, and with weights g per vertex and z per particle.

The characterization of admissible trees involves charges $q_\bullet$ and $q_\circ$ for pieces of the tree on both sides of a given inner edge. We shall refer to such pieces as *half-trees*. For convenience, we may also consider buds and leaves as half-trees, in which case we may decide to see the half-trees as dangling from the inner vertex to which they are attached. For instance, any half-tree attached to a white-empty vertex is of charge +1, whether it reduces to a leaf or it starts by a regular inner edge (see figure 4). We may then introduce the following generating functions:

(i) V for half-trees of charge 1 attached to a white-empty vertex.
(ii) S for half-trees of charge 1 attached to a white-occupied vertex.
(iii) T for half-trees of charge 4 attached to a white-occupied vertex.
(iv) R for half-trees of charge 2 attached to a black-empty vertex.

By inspecting the environments of the root vertex of these half-trees, we find the following recursion formulae, easily read off figure 7:

$$\begin{aligned} S &= 1 + 2gR & T &= -g^3 z V^4 \\ R &= gV^2 + gzS^2 + 2g^2 zT & V &= 1 + 2gR + 2g^2 zV^2 - 4g^4 z^2 V^2 S. \end{aligned} \tag{3.4}$$

The last equation may be rewritten as $(1-2g^2zV)(V-S-2g^2zVS) = 0$, hence it is equivalent to

$$V = S + 2g^2 zVS. \tag{3.5}$$

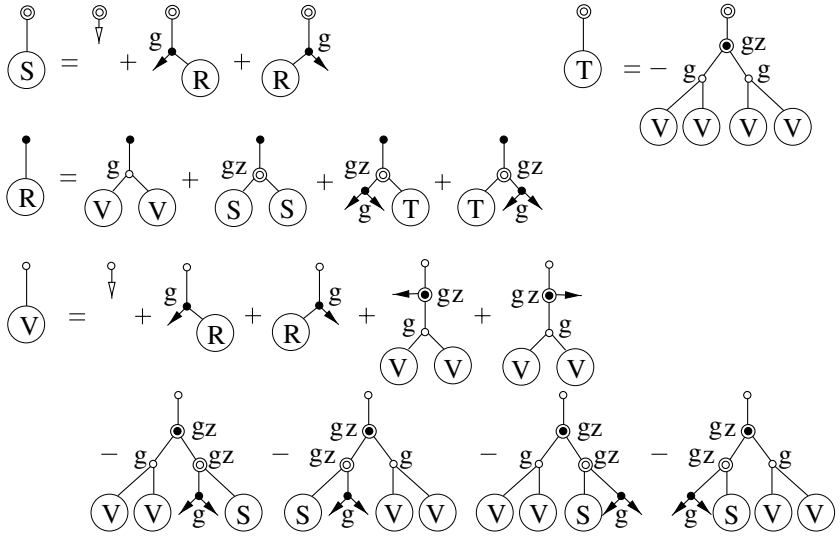

Figure 7. A pictorial representation of the recursive relations (3.4) for half-trees, respectively attached to a white-occupied vertex, with charge 1 (S) or 4 (T), to a black-empty vertex, with charge 2 (R) and to a white-empty vertex, with charge 1 (V). The various terms collect all possible environments compatible with the charge characterization of admissible trees. We also indicate the various weights g, z and minus signs.

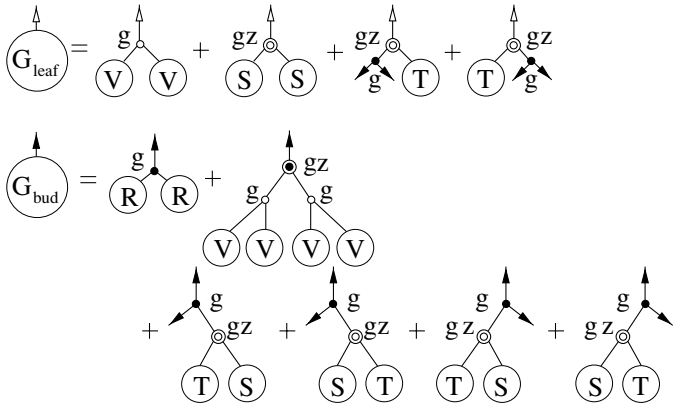

Figure 8. A pictorial representation of expressions (3.6) for G_{leaf} and G_{bud}, as obtained by collecting all possible environments of the leaf or bud compatible with the charge characterization of admissible trees. We also indicate the various weights g and z.

These equations, here derived in a purely combinatorial way, match exactly those (2.2) obtained from the matrix model solution.

Similarly, by inspection of the environment of the distinguished leaf or bud in planted trees, we immediately get the relations (see figure 8):

$$\begin{aligned} G_{\text{leaf}} &= gV^2 + gzS^2 + 2g^2zT = R \\ G_{\text{bud}} &= gR^2 + g^2z(gV^4 + 4ST). \end{aligned} \tag{3.6}$$

Equations (3.3), (3.6) and (3.4), (3.5) provide a closed system of algebraic equations for the enumeration of planar rooted bicubic maps with hard particles. The first terms of an

expansion in g of $G_{\mathrm{BMHP}}(g, z)$, counting rooted bicubic maps with, say, up to 10 vertices, read for instance

$$\begin{aligned} G_{\mathrm{BMHP}}(g,z) &= g^2(1+z) + g^4(3+9z+3z^2) + g^6(12+60z+66z^2+12z^3) \\ &\quad + g^8(56+392z+780z^2+460z^3+56z^4) \\ &\quad + g^{10}(288+2592z+7584z^2+8400z^3+3168z^4+288z^5) + \mathcal{O}(g^{12}). \end{aligned} \tag{3.7}$$

These values match exactly the general formula (2.5). The free energy F_{BMHP} is easily recovered from G_{BMHP} by inverting equation (2.4) into

$$F_{\mathrm{BMHP}}(g,z) = \frac{2}{3}\int_1^\infty \frac{\mathrm{d}u}{u} G_{\mathrm{BMHP}}\left(\frac{g}{u}, zu\right). \tag{3.8}$$

4. Cutting of rooted bicubic maps with non-sectile edges: generalities

The main theorem (3.1) is a consequence of a general relation between maps and trees obtained via some cutting procedure. In this section, we specialize to the case of planar bicubic maps without particles, but with possibly a number of distinguished *special* edges, which we prevent from being cut in the process. This general framework will be applied in the next section to the particular case of bicubic maps with hard particles by relating the special edges to NHP ones.

For starters, we first recall the cutting procedure in the standard case of bicubic maps with no special edges [11, 12]. We then extend the analysis in the presence of special *non-sectile* edges.

4.1. Preamble: cutting of ordinary bicubic maps

The cutting of a planar rooted bicubic map into a blossom tree was discussed in [11, 12]. As illustrated in figure 9, it is performed as follows:

(a) We draw the map in the plane with the external face lying to the left of its root edge (marked oriented edge originating from a black-empty root vertex) (see figure 9(*a*)).
(b) We erase the root vertex and replace the three adjacent edges by leaves. The leaf corresponding to the rooted edge is marked and taken as a root (represented as a grounding pictogram in figure 9(*b*)).
(c) Starting from this root, we visit successively each edge adjacent to the new external face in anti-clockwise direction. The edge is cut into two half-edges if (i) it originates from a black vertex and (ii) the cutting does not disconnect the remaining graph. The half-edge connected to the adjacent black vertex is replaced by a bud, while that connected to the adjacent white vertex by a leaf. This results in merging a number of faces of the original map with the external one.
(d) We iterate the cutting procedure, each time by visiting anti-clockwise the edges adjacent to the newly produced external face. We stop the process once all faces have been merged and the remaining graph is a tree (see figure 9(*d*)).

This cutting procedure is an *injection* from maps to blossom trees. Indeed, we may easily re-build the original map from its associated tree by the standard closing procedure discussed in section 3.1 (see figure 2) [11, 12]. The injection is from maps with a rooted edge (originating from a black vertex) to blossom trees with a root taken among their three unmatched leaves.

An important property of the above cutting is that it may be reformulated by use of the *geodesic distance* between faces of the map [9]. Taking the external face as origin, we may

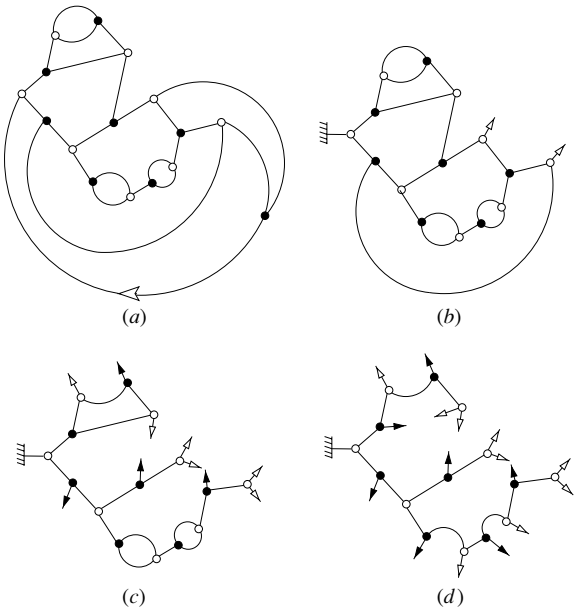

Figure 9. Cutting procedure for a typical rooted bicubic map. The various steps (*a*)–(*d*) are detailed in the text.

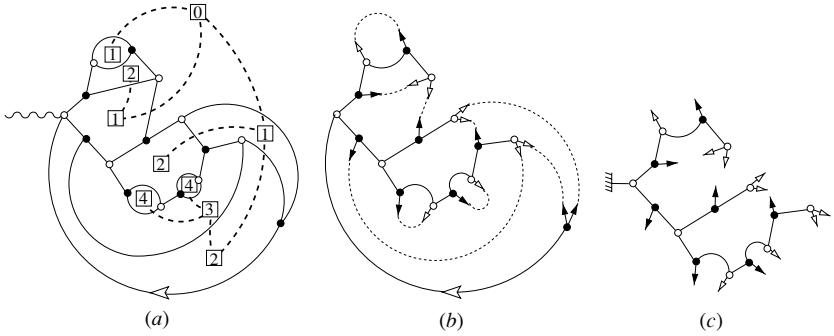

Figure 10. Equivalent formulation of the cutting procedure using geodesic distances. In (*a*), we label each face by its geodesic distance from the external face (labelled 0). Representing the seam by a wavy line, the geodesic tree, made of all leftmost minimal paths is drawn in dashed lines. The edges dual to those of this tree are replaced in (*b*) by bud–leaf pairs. The blossom tree is finally obtained by erasing the root edge and root vertex (*c*), replacing them by the root of the tree.

define its geodesic distance to any other face of the map as the minimal number of edges to be crossed by a path stepping from face to face from the external face to the face at hand. The paths are further required (i) to leave black vertices on their left, and (ii) not to cross a seam connecting the extremity of the rooted edge to infinity. Such paths realizing the minimal number of steps are called minimal paths. Any two such paths P_1 and P_2 may be ordered by comparing their first differing steps s_1 and s_2. The path P_1 is said to lie on the left of P_2 if s_1 lies on the left of s_2, looking towards the map from infinity. This ordering allows us to assign to each face its *leftmost minimal path*. The union of these paths for all faces forms a 'geodesic tree' (see figure 10(*a*)). The above cutting procedure may be rephrased by cutting the edges

dual to those of the geodesic tree and replacing them by bud–leaf pairs (see figure 10(*b*)). The original root edge and root vertex are removed together with the attached buds and replaced by a distinguished leaf (see figure 10(*c*)).

The image of bicubic maps under cutting has the simple charge characterization that all edges be regular, as will be re-derived below. This allows for a nice bijective census of these maps.

4.2. Cutting procedure in the presence of non-sectile edges

The above cutting procedure is a particular case of a more general cutting which also allows for the presence of *non-sectile* edges within the map. More precisely, we may pick in a bicubic map a number of *special* edges which we decide *a priori* not to cut. Edges which are not special will be called *normal*. We can repeat the above cutting process following the same rules (*a*)–(*d*) of section 4.1, but with the extra requirement that special edges should not be cut. There is no guarantee in general that the cutting process may be carried on so as to produce a tree. In the following, we shall therefore restrict ourselves to *acceptable* choices of special edges, i.e. such that the cutting procedure does indeed produce a tree. In other words, we forbid any choice of special edges for which a face of the map would be surrounded only by special edges and white-to-black edges anti-clockwise. We also forbid special edges to be adjacent to the root vertex of the map. From now on, we shall always consider maps with an acceptable choice of special edges.

The presence of special edges allows for the definition of a *new geodesic distance* using paths with the same requirements as before, namely that (i) these paths leave black vertices on their left and (ii) do not cross a seam connecting the extremity of the rooted edge to infinity and with the additional requirement that (iii) they now avoid the special edges. A choice of special edges is acceptable if and only if each face remains at a finite distance from the external face. Moreover, the cutting procedure in the presence of special edges may still be rephrased as cutting the edges dual to those of the geodesic tree made of all leftmost minimal paths (from the external face to all other faces) that avoid the special edges. A typical example of cutting procedure with special edges is displayed in figure 11.

We now wish to characterize the trees obtained by the above cutting. Clearly, by construction, any such tree satisfies the following properties.

(S1) Its inner vertices are of two types: black or white vertices, all with valence three. Its inner edges are of two types, normal or special.
(S2) It is bicoloured, i.e. all its inner edges connect only black to white vertices.
(S3) It has two kinds of leaves: buds, connected only to black inner vertices and leaves, connected only to white ones.
(S4) Its total charge (no. of leaves $-$ no. of buds) is equal to 3.
These are nothing but properties (1)–(4), i.e. the tree is indeed a blossom tree as defined in section 3.1. The tree further enjoys the following charge characterization:
(S5) Normal (i.e. non-special) edges are regular.

From properties (S1)–(S4), this last property may be rephrased into:

(S5′) Normal edges are of type $(q_\circ : q_\bullet)$ with $q_\circ \geqslant 2$ and $q_\bullet \leqslant 1$.

Properties (S1)–(S4) are obvious. Let us now show property (S5). Recall that, as is true for any blossom tree, we have $q_\circ \equiv 2 \bmod 3$ and $q_\bullet \equiv 1 \bmod 3$ for the charge on both sides of any inner edge e. Moreover, these charges may be related to geodesic distances as follows. Let us denote respectively by k and m the geodesic distances of the two faces (resp. κ and μ) adjacent

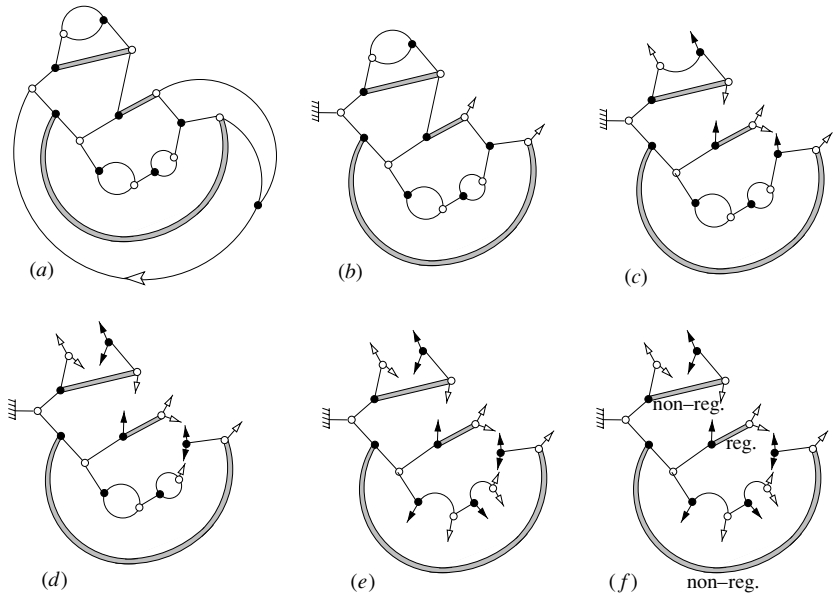

Figure 11. A typical example of cutting of a rooted bicubic map (*a*) with special, non-sectile edges, represented by thickened grey lines. In (*b*), we have erased the root vertex of the map and replaced the adjacent edges by leaves, the extremity of the rooted edge serving as a root (grounding pictogram). We iterate the standard cutting procedure (*c*)–(*e*) without cutting the special edges until a tree is obtained (*e*). That the cutting ends up with a tree is guaranteed by the absence of anti-clockwise loops of either special or white-to-black edges. All non-special edges are regular but special edges may be regular or non-regular (*f*).

to e on the original map, with the convention that the face μ follows the face κ anti-clockwise around the black endpoint of e (see figure 12). As a consequence of the leftmost minimal path formulation of the cutting, we may relate the charges $q_\circ$ and $q_\bullet$ of the two pieces of the tree on both sides of e to the geodesic distances k and m. Suppose for instance a situation like that of figure 12 in which the three unmatched leaves of the tree all lie on the same side of e, that of its black endpoint. Denoting the piece of the tree on this side by $\mathcal{T}_1$ and by $\mathcal{T}_2$ the piece on the side of the white endpoint of e, suppose moreover that the root is the last of the three unmatched leaves encountered by turning clockwise around $\mathcal{T}_1$ from e. Then the leftmost minimal path leading to μ will cut m edges, resulting in the creation of m leaves in $\mathcal{T}_1$ among which $m - p$ are matched to buds in $\mathcal{T}_2$, and p are matched to buds of $\mathcal{T}_1$ by edges turning around $\mathcal{T}_2$ (see figure 12). The leftmost minimal path leading to κ has to cross these p edges plus $k - p$ other edges, thus resulting in the creation of $k - p$ leaves in $\mathcal{T}_2$ matched to $k - p$ buds in $\mathcal{T}_1$. All other bud–leaf pairs correspond to cut edges not crossed by the two leftmost minimal paths we are considering and thus lie on the same side of e on the tree, giving a net contribution zero to the charges of either piece. The charge of $\mathcal{T}_1$ is therefore $q_\bullet = 3 + m - k$ while the charge of $\mathcal{T}_2$ is $q_\circ = k - m$. There are 12 possible relative positions of the three unmatched leaves in either piece, as displayed in figure 13. A detailed case by case inspection of these 12 cases shows that $q_\circ = k - m$ if the root of the tree lies on the side of the black endpoint of e and $q_\circ = 3 + k - m$ if it lies on the side of the white endpoint.

Finally, to prove (S5), we further assume that the edge e is normal. The fact that it was not cut in the cutting process implies some inequality on the geodesic distances k and m. Indeed, we must have $m \leqslant k + 1$ to eliminate the possibility of a shorter path leading to μ by crossing

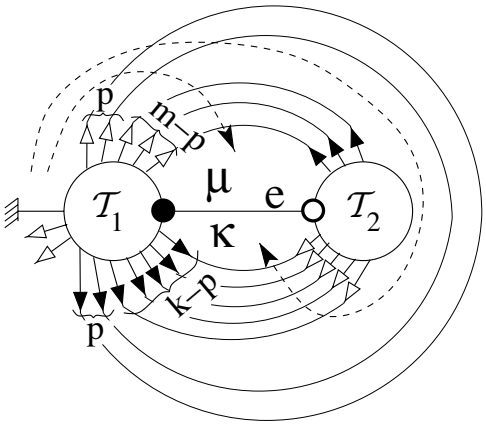

Figure 12. Relation between the charges $q_\bullet$ and $q_\circ$ of the two pieces of tree $\mathcal{T}_1$ and $\mathcal{T}_2$ on both sides of an edge e, and the geodesic distances m and k from the external face of the two faces μ and κ adjacent to e on the map. We use the convention that the face μ follows the face κ anti-clockwise around the black endpoint of e. We picked a particular configuration of the three unmatched leaves of the tree, here all lying in $\mathcal{T}_1$. We read from the picture $q_\circ = (k-p)-(m-p) = k-m$, hence $q_\bullet = 3+m-k$.

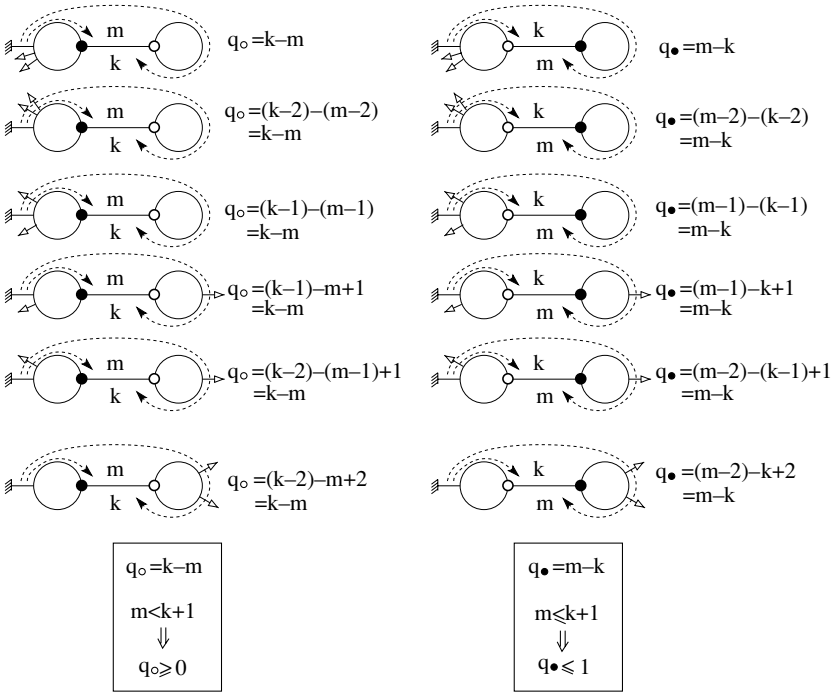

Figure 13. Relation between the charges $q_\bullet$ and $q_\circ$ of the two pieces of tree on both sides of an edge, and the geodesic distances m and k from the external face of the two faces adjacent to this edge on the map. We use the convention that the face at distance m follows that at distance k anti-clockwise around the black endpoint of the edge. There are 12 possible relative positions for the three unmatched leaves of the tree. In all cases on the left, we find $q_\circ = k-m$ while on the right $q_\bullet = m-k$. The absence of leftmost minimal path crossing the edge imposes inequalities on the geodesic distances k and m as shown. These inequalities translate into $q_\circ \geqslant 0$ or $q_\bullet \leqslant 1$.

e from κ. As the leftmost minimal path leading to μ lies on the right of that leading to κ when the root lies on the side of the black endpoint of e, we must further forbid $m = k + 1$ in this case to eliminate the possibility of a path of the same length, but more to the left, by crossing e (see figure 13). These inequalities, together with the relations above between k, m and the charges $q_\circ$ and $q_\bullet$ immediately lead to the inequalities $q_\circ \geqslant 0$ or $q_\bullet \leqslant 1$. Combining this with $q_\circ = 3 - q_\bullet \equiv 2 \bmod 3$, we deduce (S5′), or equivalently (S5), i.e e is regular. Note that there is no such characterization for special edges which may be regular or not (see figure 11(f)).

To conclude this section, let us insist on property (S5) (S5′) which we rephrase as

Proposition C1. *If a tree $\mathcal{T}$ is obtained by the cutting of a map $\mathcal{M}$ with a number of special (non-sectile) edges, then all normal (*a priori *sectile) edges of $\mathcal{T}$ are regular. Equivalently, if an edge of $\mathcal{T}$ is non-regular, it must be a special edge.*

4.3. Closing-cutting procedure: bijection

The above cutting procedure sends any planar rooted bicubic map with an acceptable choice of special edges onto a rooted blossom tree with special edges and with the properties (S1)–(S5) above. This correspondence is clearly injective as the map is easily restored from the tree by the same closing algorithm as that discussed in section 3.1. Moreover, as we shall now see, the properties (S1)–(S5) entirely characterize the image of the maps under cutting. We have therefore a bijection between, on one hand, planar rooted bicubic maps with acceptable choices of special edges and, on the other hand, blossom trees with special edges satisfying properties (S1)–(S5), and with a distinguished leaf among their three unmatched ones. That the closing of such a tree builds a rooted bicubic map with special edges is obvious. That the corresponding choice of special edges is acceptable is also clear as each face of the map is attainable from the external face by a path whose edges are dual to the closing arches plus possibly the duals of some edges adjacent to the root vertex of the map. We are now left with the task of showing that closing a tree $\mathcal{T}$ with the above properties into a map $\mathcal{M}$ with the same special edges and re-opening it via the cutting procedure that preserves these special edges rebuilds $\mathcal{T}$. It is clear that the cutting procedure produces a tree $\mathcal{T}'$ satisfying (S1)–(S5) and with the same number of inner vertices as $\mathcal{T}$, thus the same number of inner edges. To prove that $\mathcal{T} = \mathcal{T}'$, it is thus sufficient to prove that all the inner edges of $\mathcal{T}$ are in $\mathcal{T}'$. It is clear that the special edges of $\mathcal{T}$ and $\mathcal{T}'$ are the same as they are not affected by the closing–cutting process. It is therefore sufficient to show that no normal edge of $\mathcal{T}$ may be cut in the cutting process. Assuming the contrary, let us pick a normal edge e of $\mathcal{T}$, supposedly cut in the cutting process and with the *minimal distance* in $\mathcal{M}$ from the external face. By such edge distance, we mean the distance of that of the two faces, say κ, adjacent to e such that the black vertex lies on the left when crossing e from that face. We denote by k this distance and by m the *depth* of the other face, say μ adjacent to e in $\mathcal{M}$. By depth, we mean the number of closing arches (plus possibly the number of edges adjacent to the root vertex of $\mathcal{M}$) separating μ from the external face in the closing process of $\mathcal{T}$. Clearly, a path of length m exists on $\mathcal{M}$ from the external face to μ. The fact that e is cut by a leftmost minimal path then imposes that $k + 1 \leqslant m$, and moreover that $k + 1 < m$ if the root of $\mathcal{T}$ lies on the side of the white vertex adjacent to e (see figure 14). Note finally that, since we have chosen an edge with the minimal distance, the leftmost minimal path from the external face to κ cannot cut any edge of $\mathcal{T}$, thus k is also the depth of κ (as defined above) in the closing process of $\mathcal{T}$. This allows us to relate k and m to the charges of the two pieces of $\mathcal{T}$ on both sides of e, namely $k - m = q_\circ$ if the root of $\mathcal{T}$ lies on the side of the black endpoint of e or $m - k = q_\bullet$ if it lies on the side of the white endpoint of e (see figure 14). The above inequalities on k and m translate into $q_\circ \leqslant -1$, or

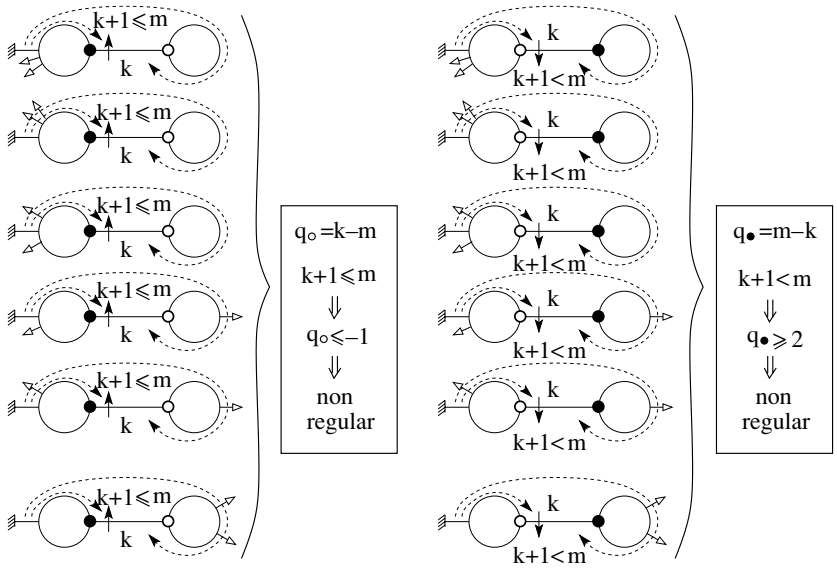

Figure 14. The cutting of a normal, thus necessarily regular edge, of $\mathcal{T}$ by a leftmost minimal path crossing that edge implies inequalities between the distance k of the face adjacent to that edge (and such that the black endpoint lies on the left when crossing the edge from that face) and the depth m of the other adjacent face in the closing process of $\mathcal{T}$ (number of arches encircling that face). If we have picked an edge with minimal k, k is also the depth of the first face in the closing process of $\mathcal{T}$ and we may relate m and k to the charges $q_\circ$ and $q_\bullet$ of the two halves of the tree as shown. The inequalities then translate into the fact that the edge is not regular, a contradiction.

equivalently $q_\bullet \geqslant 2$ (see figure 14), which implies that e is non-regular, hence contradicting (S5). We deduce that normal edges of $\mathcal{T}$ are not cut, hence $\mathcal{T} = \mathcal{T}'$ as announced.

To conclude this section, let us note that a direct outcome of the above proof are the following statements:

Proposition C2. *Starting from a blossom tree with regular and non-regular edges, if we wish to recover the same tree in a closing–cutting procedure, it is necessary and sufficient to impose that all the non-regular edges of the tree be marked as non-sectile. Indeed, all regular edges will remain uncut, even if their cutting is* a priori *allowed.*

Proposition C3. *If the cutting of a map $\mathcal{M}$ with special edges creates a tree $\mathcal{T}$ in which some of the special edges are regular, then in each cutting of $\mathcal{M}$ for which some of these edges are no longer marked as special on $\mathcal{M}$ (i.e. become* a priori *sectile), the latter remain uncut, hence we obtain the same tree $\mathcal{T}$, but with fewer regular special edges.*

5. Application to bicubic maps with hard particles: proof of main theorem

We are now ready to prove our main result (3.1).

5.1. Admissible maps and equivalence classes of admissible trees

We start with our family of admissible trees $\mathcal{T}$ as defined by (1)–(6). In particular, the regular edges match exactly the HP ones, while the non-regular edges match exactly the doubly occupied ones. We define an *admissible map* as any rooted planar bicubic map $\mathcal{M}$ with

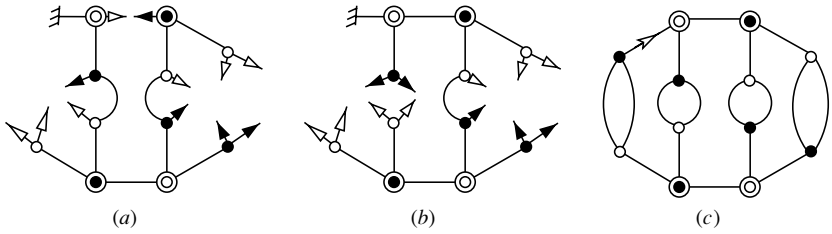

Figure 15. An example of two admissible trees (*a*) and (*b*) in the same equivalence class, i.e. whose closing builds the same admissible map (*c*). Note that the closing of (*a*) has created on the map (*c*) one more NHP edge than that originally on the tree.

particles obtained by the closing of an admissible tree $\mathcal{T}$. A given admissible map may in general be obtained by the closing of several admissible trees (see figure 15). This leads us naturally to define an *equivalence relation* among admissible trees, by $\mathcal{T} \sim \mathcal{T}'$ if and only if they lead to the same map $\mathcal{M}$. The corresponding equivalence class is denoted by $\mathcal{C}_{\mathcal{M}}$. We shall now rely on propositions C1–C3 above to characterize equivalence classes.

Starting from an admissible tree $\mathcal{T} \in \mathcal{C}_{\mathcal{M}}$, we may decide to mark as special edges on $\mathcal{T}$ *all its non-regular NHP edges*, keeping all regular HP edges as normal edges. The tree $\mathcal{T}$, together with these special edges, satisfies property (S5). Moreover, the marking of special edges of $\mathcal{T}$ induces a marking of special edges on $\mathcal{M}$ which are necessarily NHP on $\mathcal{M}$. Note that $\mathcal{M}$ has in general more NHP edges than those of $\mathcal{T}$, as doubly occupied edges may be created in the closing process (see figure 15). Still, according to proposition C2, the tree $\mathcal{T}$ is recovered from $\mathcal{M}$ by the cutting process avoiding the special edges. We immediately deduce that any tree in $\mathcal{C}_{\mathcal{M}}$ is obtained from a particular cutting of $\mathcal{M}$ in which a number of its NHP edges have been marked as special. Sweeping all possible such marking of NHP edges on $\mathcal{M}$, we get of course in general many more trees than those of $\mathcal{C}_{\mathcal{M}}$ as some choices of NHP edges on $\mathcal{M}$ may lead to trees which are not admissible.

5.2. Cutting of admissible maps

Let us now discuss precisely the cutting of an admissible map $\mathcal{M}$. Denoting by NHP($\mathcal{M}$) its set of NHP edges with cardinality $m \equiv m(\mathcal{M}) = |\mathrm{NHP}(\mathcal{M})|$, we are led to consider the 2^m different cuttings corresponding to the 2^m possible choices of special edges among the doubly occupied ones. Each cutting amounts to the choice of a subset $\mathcal{S} \subset \mathrm{NHP}(\mathcal{M})$ with cardinality $p \equiv p(\mathcal{S}) = |\mathcal{S}|$. For any such choice $\mathcal{S}$, the cutting process results in a tree, i.e. the marking is acceptable. Indeed, a non-acceptable choice would require to have a loop made, anti-clockwise, of either special, hence doubly occupied edges or white-to-black edges. As black and white alternate along a loop, we would deduce the presence of a loop made of occupied particles only. This is clearly impossible as, from the environment of a NHP edge on admissible trees (see figure 5), a NHP edge is always followed or preceded by a HP edge on the side of its doubly occupied black vertex. Note also that, as it should, the special edges cannot be adjacent to the root vertex of the map as the latter is unoccupied. Moreover, the obtained tree $\mathcal{T}$ satisfies properties (S1)–(S5), from which we immediately deduce properties (1)–(5) of admissible trees. In particular, if an edge is non-regular, it must be special according to (S5), hence it must be doubly occupied. In other words, HP edges on $\mathcal{T}$ are necessarily regular, which is nothing but (5) or equivalently (5′). In general however, property (6) of admissible trees is not guaranteed, i.e. the tree may have a number of NHP regular edges. Let us now discuss the various situations which may occur:

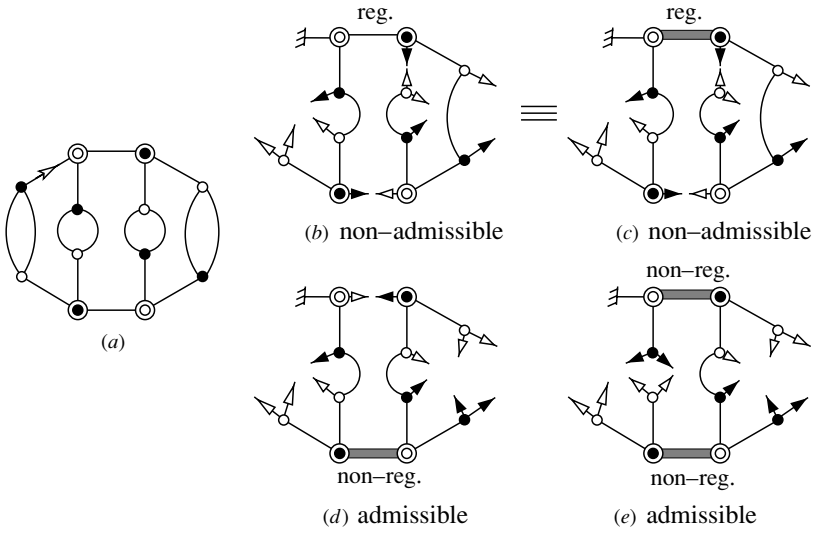

Figure 16. The $2^m = 4$ cuttings of the admissible map $\mathcal{M}$ in (*a*) with $m = 2$ NHP edges. Three different trees are obtained. A non-admissible tree with $r = 1$ is obtained for the $2^r = 2$ cuttings (*b*) and (*c*) corresponding to marking or not the upper horizontal doubly occupied edge. The two other possible markings where the lower horizontal doubly occupied edge is marked and the upper horizontal doubly occupied edge is marked or not lead to two different admissible trees (*e*) and (*f*). The equivalent class $\mathcal{C}_{\mathcal{M}}$ is made of these two trees. As one of them has one NHP inner edge and the other two, their contributions with a weight -1 per NHP inner edge add up to 0.

(i) $m = 0$. Then the map satisfies the hard-particle constraint. The corresponding equivalence class is made of the unique tree $\mathcal{T}$ obtained by cutting $\mathcal{M}$ with no special edges. This tree $\mathcal{T}$ is a good tree.

(ii) $m > 0$. Then the map does not satisfy the hard-particle constraint. The corresponding equivalence class is made of admissible trees which are all obtained by cuttings of $\mathcal{M}$ with a subset of its NHP edges marked as special.

In this case (ii), and for a given choice $\mathcal{S}$ among the 2^m possible subsets of NHP($\mathcal{M}$), let us further denote by $r \equiv r(\mathcal{T})$ the number of NHP regular edges of the resulting tree $\mathcal{T}$ and by $n \equiv n(\mathcal{T})$ its number of NHP non-regular ones. We clearly have $n \leqslant p$ as non-regular edges are necessarily special, and also $p \leqslant n + r$ as all special edges are NHP edges of $\mathcal{T}$. Now again two situations may occur:

(iia) $r = 0$. Then all NHP edges are non-regular, i.e. property (6) is satisfied and the tree $\mathcal{T}$ is admissible. In this case, the above inequalities moreover imply that $n = p$, i.e. the NHP edges of $\mathcal{T}$ are exactly the marked NHP edges of $\mathcal{M}$. Note that, from proposition C1, the marking $\mathcal{S}$ at hand then corresponds to the *only* choice (among the 2^m) that leads to the admissible tree $\mathcal{T}$.

(iib) $r > 0$. In this case, the tree $\mathcal{T}$ is not admissible. From proposition C3, we also know that the 2^r choices corresponding to

- marking as special on $\mathcal{M}$ all the NHP non-regular edges of $\mathcal{T}$,
- marking or not the NHP regular edges,

all lead to the same tree $\mathcal{T}$. From proposition C1, these 2^r markings are the *only* choices (among the 2^m) that lead to $\mathcal{T}$.

Figure 16 shows an example of the $2^m = 4$ cuttings of an admissible map with $m = 2$ doubly occupied edges. The resulting trees are two admissible trees, each obtained for a unique

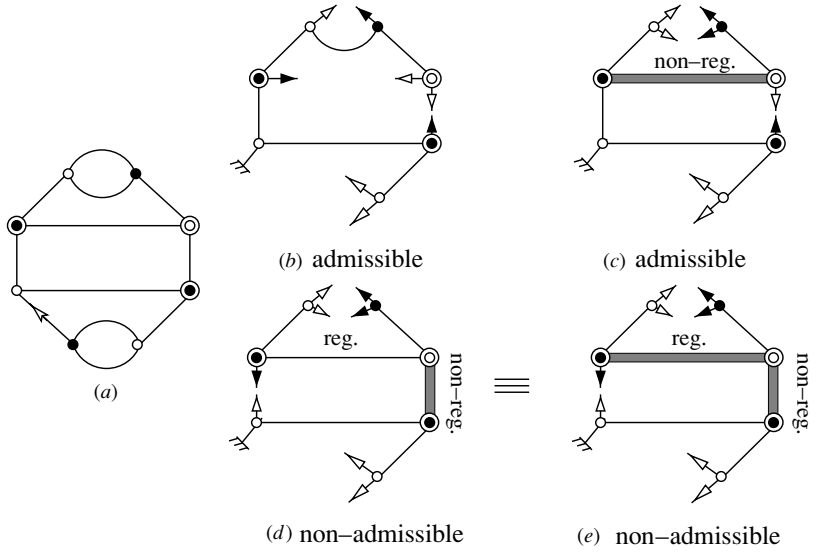

Figure 17. The $2^m = 4$ cuttings of another admissible map $\mathcal{M}$ in (a) with $m = 2$ NHP edges. Again the class $\mathcal{C}_\mathcal{M}$ is made of two trees (b) and (c) whose contribution with a weight -1 per NHP edge add up to 0. The tree in (d) is identical to that in (e). It has $r = 1$ and is obtained by the $2^r = 2$ markings of the original map where the vertical doubly occupied edge is selected and the horizontal one is either marked or not. As opposed to the case of figure 16, the cutting with no marking (b) leads to an admissible tree.

choice of special NHP edges on $\mathcal{M}$, and a non-admissible tree with $r = 1$ obtained for $2^r = 2$ choices of special NHP edges on $\mathcal{M}$. The class $\mathcal{C}_\mathcal{M}$ is thus made of two elements. Another similar example is displayed in figure 17.

5.3. Sum rule and proof of main theorem

We may now derive the sum rule (3.1) as follows. We start with an admissible map $\mathcal{M}$ with $n_\circ$ white-empty particles, $n_\bullet + 1$ black-empty particles, $n_\circledcirc$ white-occupied particles and $n_\odot$ black-occupied particles. We then sum over the $2^{m(\mathcal{M})}$ choices $\mathcal{S}$ of markings of NHP edges as special edges. We assign to each choice a weight $(-1)^{p(\mathcal{S})}$, i.e. a weight -1 per marking. We have clearly

$$\sum_{\mathcal{S}\subset \mathrm{NHP}(\mathcal{M})} (-1)^{p(\mathcal{S})} = \delta_{m(\mathcal{M}),0} \times 1 + (1 - \delta_{m(\mathcal{M}),0})(1 + (-1))^{m(\mathcal{M})}$$
$$= \delta_{m(\mathcal{M}),0} \tag{5.1}$$

as when $m(\mathcal{M}) = 0, \mathcal{S} = \mathrm{NHP}(\mathcal{M}) = \emptyset$ and, when $m(\mathcal{M}) > 0$, each NHP edge may independently be marked or not. Alternatively we may reorganize the same sum by regrouping all subsets $\mathcal{S}$ that lead upon cutting to the same tree $\mathcal{T}$ (admissible or not) and write

$$\sum_{\mathcal{S}\subset \mathrm{NHP}(\mathcal{M})} (-1)^{p(\mathcal{S})} = \sum_{\mathcal{T}} \sum_{\substack{\mathcal{S}\ \text{leading} \\ \text{to}\ \mathcal{T}}} (-1)^{p(\mathcal{S})}$$
$$= \sum_{\substack{\mathcal{T}\ \text{s.t.} \\ r(\mathcal{T})=0}} (-1)^{n(\mathcal{T})} + \sum_{\substack{\mathcal{T}\ \text{s.t.} \\ r(\mathcal{T})>0}} (-1)^{n(\mathcal{T})}(1 + (-1))^{r(\mathcal{T})}$$
$$= \sum_{\mathcal{T}\in\mathcal{C}_\mathcal{M}} (-1)^{n(\mathcal{T})} \tag{5.2}$$

where the sums in the first two lines extend over all trees $\mathcal{T}$ resulting from all cuttings of $\mathcal{M}$. These trees satisfy properties (1)–(5) of admissible trees, but do not satisfy (6) in general. We have also used the fact that admissible trees are those with $r(\mathcal{T}) = 0$ and the fact that, in this case, $n(\mathcal{T}) = p(\mathcal{S})$ (cases (i) or (iia) above) while trees having $r(\mathcal{T}) > 0$ are obtained in $2^{r(\mathcal{T})}$ ways corresponding to marking all their non-regular NHP edges and marking or not independently each regular NHP edge. Comparing equations (5.1) and (5.2) leads directly to the sum rule

$$\sum_{\mathcal{T}\in\mathcal{C}_{\mathcal{M}}} (-1)^{n(\mathcal{T})} = \delta_{m(\mathcal{M}),0}. \tag{5.3}$$

As $m(\mathcal{M}) = 0$ precisely means that the map satisfies the hard-particle constraint, the rhs above is nothing but the characteristic function of rooted bicubic maps with hard particles within the larger set of admissible maps. Summing over all admissible maps $\mathcal{M}$, we immediately deduce the main theorem (3.1).

6. Discussion

In this paper, we have presented a direct combinatorial derivation of the generating function for hard particles on planar bicubic maps by the use of admissible trees. To conclude, we shall first briefly present yet another application of our construction to the Ising model on tetravalent maps, described by a similar chain-interacting four-matrix integral. More generally, our construction may be extended to models of maps with particles subject to exclusion rules, all described, as mentioned in the introduction, by chain-interacting multi-matrix integrals. We shall sketch below the general structure of admissible trees for the general multi-matrix case. We will finally comment on the predicted existence of an Ising-like crystallization transition for a particular model of trees with particles, with possible re-interpretation as a branching process.

6.1. The Ising model revisited

The Ising model on tetravalent maps is well known to be described by a two-matrix integral with quartic potential. For the present purpose however, it is more instructive to view it as a hard-particle model on bipartite maps, hence described by a four-matrix integral. More precisely, let us consider hard particles on bipartite planar maps with bi- and tetravalent vertices only and with the constraint that all tetravalent vertices are unoccupied, while all bivalent ones are occupied. In the matrix language, the corresponding action reads

$$U(M_1, \ldots, M_4) = M_1M_2 - M_2M_3 + M_3M_4 - g\left(\frac{M_1^4}{4} + \frac{M_4^4}{4}\right) - gz\left(\frac{M_2^2}{2} + \frac{M_3^2}{2}\right) \tag{6.1}$$

with four matrices describing black-empty tetravalent (M_1), white-occupied bivalent (M_2), black-occupied bivalent (M_3) and white-empty tetravalent (M_4) vertices and with a weight g per vertex and z per particle. The Ising model is recovered by erasing all bivalent vertices. This results in tetravalent maps with black and white vertices, all with weight g, linked irrespectively of their colour, but with an effective edge coupling 1 for edges adjacent to vertices of opposite colour and gz for edges adjacent to vertices of the same colour. This is nothing but the Ising model upon interpreting colours as spins.

Returning to our bipartite hard-particle formulation, it proves convenient to consider maps with a single additional bivalent black-empty root vertex. This corresponds to what was called 'quasi-tetravalent' maps in [14]. The corresponding maps may be enumerated along the same

lines as above by counting properly signed admissible trees. An admissible tree is now defined as follows:

(1) Its inner vertices are of four types: black or white vertices, each of which being either empty or occupied by a particle. All empty vertices have valence four and all occupied ones have valence two.
(2) It is bicoloured, i.e. all its inner edges connect only black (empty or occupied) inner vertices to white (empty or occupied) ones.
(3) It has two kinds of leaves: the so-called buds, connected only to black (empty or occupied) inner vertices and the so-called leaves, connected only to white (empty or occupied) inner vertices. We attach a *charge* -1 to each bud and a charge +1 to each leaf.
(4) Its total charge (no. of leaves − no. of buds) is equal to 2.
(5) All HP edges of the tree are regular.
(6) All NHP edges of the tree are non-regular.

As a consequence of (1)–(4), any inner edge separates the tree into a piece of total charge $q_\circ \equiv 1 \bmod 2$ starting with a white vertex, and a piece of total charge $q_\bullet = 2 - q_\circ \equiv 1 \bmod 2$ starting with a black vertex. Such an edge will be again called of type $(q_\circ : q_\bullet)$. As before, the last two characterizations (5) and (6) may be rephrased into

(5′) Every HP edge is of type $(q_\circ : q_\bullet)$ with $q_\circ \geqslant 1$, hence $q_\bullet \leqslant 1$.
(6′) Every NHP edge is of type $(q_\circ : q_\bullet)$ with $q_\circ \leqslant -1$, hence $q_\bullet \geqslant 3$.

A detailed survey of possible local environments shows that admissible trees have only NHP edges of type $(q_\circ = -1 : q_\bullet = 3)$, while HP edges are of type $(q_\circ = 3 : q_\bullet = -1)$ or $(q_\circ = 1 : q_\bullet = 1)$. As before, the generating function G_{QTIsing} of quasi-tetravalent maps with Ising spins is expressed as that of admissible trees with a weight -1 per NHP edge. The latter is easily obtained from the generating function of planted trees, expressed in terms of generating functions for half trees. The half trees to be considered are

(i) half-trees of charge -1 attached to a white-occupied vertex, generated by A,
(ii) half-trees of charge 1 attached to a white-occupied vertex, generated by B,
(iii) half-trees of charge 3 attached to a white-occupied vertex, generated by C,
(iv) half-trees of charge 1 attached to a black-empty vertex, generated by R,
(v) half-trees of charge 3 attached to a black-empty vertex, generated by S,
(vi) half-trees of charge -1 attached to a white-empty vertex, generated by U,
(vii) half-trees of charge 1 attached to a white-empty vertex, generated by V.

These functions satisfy recursion relations, obtained by inspection of the environment of the root, as displayed in figure 18:

$$\begin{aligned} A &= 3gR & B &= 1 + 3gR^2 + 3gS \\ C &= -g^2zV^3 & R &= 3gV^2U + gzB \\ S &= gV^3 + gzC & U &= 3gR + gz - g^2z^2A \\ V &= 1 + 3gR^2 + 3gS + 3g^2zV^2U. \end{aligned} \tag{6.2}$$

The generating function G_{QTIsing} is easily related to the above, now via

$$G_{\mathrm{QTIsing}}(g, z) = gR - g^2(R^3 + 6RS + gzV^3) \tag{6.3}$$

obtained by attaching admissible trees to either a leaf (first contribution) or a bud (second contribution with minus sign). To make the connection with previous results on the Ising

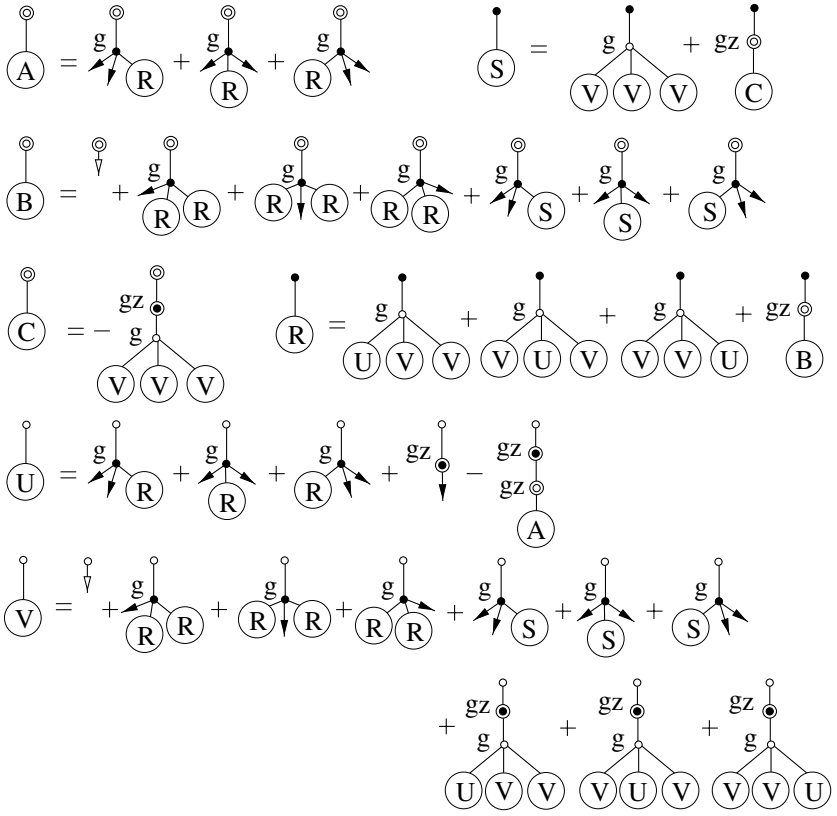

Figure 18. A pictorial representation of the recursive relations (6.2) for half-trees, respectively attached to a white-occupied vertex, with charge -1 (A), 1 (B) or 3 (C), to a black-empty vertex, with charge 1 (R) or 3 (S) and to a white-empty vertex, with charge -1 (U) or 1 (V). The various terms collect all possible environments compatible with the charge characterization of admissible trees. We also indicate the various weights g, z and minus signs.

model, we note that, by elimination, system (6.2) reduces to a single algebraic equation for V, which, upon the substitutions $P = V/(1 - g^2z^2)$, $x = g(1 - g^2z^2)^2$ and $v = gz$, reads

$$P = 1 + 3x^2P^3 + v^2\frac{P}{(1 - 3xP)^2}. \tag{6.4}$$

This equation is nothing but that of [14, 31]. We also easily check that formula (6.3) matches that of [14].

6.2. Generalizations

The construction of this paper may be extended so as to describe hard particles on bipartite maps with vertices of arbitrary valences (arbitrary polynomial potential for each matrix in the action). In this case, the admissible trees themselves have arbitrary valences. Again their fundamental characterization is that HP edges have to be regular while NHP ones have to be non-regular. A weight -1 per NHP edge is still required to perform the right counting.

More interestingly, the method can easily be extended to describe particles with exclusion rules on bipartite maps. As discussed in the introduction, we may impose that each edge have a total number of adjacent particles of at most k, corresponding to a multi-matrix integral over

$2k + 2$ matrices. Very generally, the tree formulation will use admissible trees with vertices occupied by at most k particles, and whose edges either satisfy the exclusion rule (ER edges) or do not (NER edges). The admissible trees are now required to have all their ER edges regular and all their NER ones non-regular. For maps with bounded valences, the number of allowed $(q_\circ : q_\bullet)$ pairs will remain finite, hence the number of half-trees to be dealt with is finite as well. To recover the correct generating function for the maps, we simply have to include again a weight -1 per NER edge. In practice, the enumeration might prove cumbersome, although straightforward. An example with $k = 2$ of a six-matrix model which displays the tricritical Ising transition was solved in [29] by matrix techniques. The corresponding algebraic equations may be easily re-interpreted in terms of generating functions for (signed) admissible half-trees. The case on non-bipartite maps is more subtle and so far, we only know how to treat the case of odd $k = 2p + 1$ upon transforming its configurations into those of bipartite maps with edges adjacent to at most p particles.

6.3. Trees with Ising transition

The generating function G_{BMHP} of planar bicubic maps with hard particles, rooted at a black-empty vertex is also that of good trees (up to a multiplicative factor g for the removed root vertex). Recall that we may view the good trees as those obeying:

(G1) the hard-particle constraint is satisfied on the tree,

(G2) properties (1) to (5) of sections 3.1 and 3.2 hold,

(G3) the closing of the tree produces a map satisfying the hard-particle constraint.

These trees are moreover rooted at one of their three unmatched leaves. We may as well consider the same trees, but now planted at *any* of their leaves, and generated by G_{leaf}. From the relation $G_{\mathrm{leaf}} = R$, apparent from figures 7 and 8, we can interpret R as generating *planted good trees* satisfying properties (G1)–(G3), with weights g per vertex and z per particle. In particular, as we restrict ourselves to good trees *ab initio*, no sign factors are required. We have the relation

$$G_{\mathrm{BMHP}}|_{g^{2n}} = \frac{3}{n+2} R|_{g^{2n-1}} \tag{6.5}$$

between the coefficients in g of the two series, expressing that only 3 of the $n + 2$ available leaves are unmatched in good trees with $2n - 1$ vertices. Note also that property (5) may be rephrased into: all descending subtrees of a planted good tree have charge $q_\bullet = 1$ if they start by a black vertex, and charge $q_\circ = 2$ if they start by a white vertex.

Alternatively, we may also interpret S as counting a slightly different version of planted good trees obtained as follows. Starting from a planar bicubic map with hard particles rooted at a black-empty vertex, and using the cutting process of figure 10 based on the geodesic tree, we may stop the process at step (b), i.e. keep the root vertex and its two attached buds and plant the tree at one of these buds. The resulting tree is a new type of planted good tree satisfying the following properties (G1′)–(G3′). Property (G1′) is the same as (G1). Property (G2′) is similar to (G2) but with (4) replaced by: its total charge is 0 and with (5) replaced by: all descending subtrees have charge $q_\bullet = 1$ if they start by a black vertex, and charge $q_\circ = 2$ if they start by a white vertex. Finally (G3′) states that closing the tree into a map by simply connecting iteratively all successive bud–leaf pairs produces a map with no NHP edge. It is then easy to see that these planted trees, with weights g per vertex and z per particle are generated by S, as apparent from figure 7 by replacing the white-occupied root vertex of S by

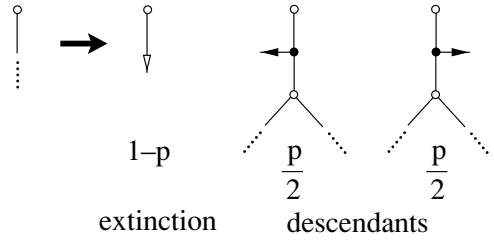

Figure 19. Local evolution rules for the branching process associated with good trees without particles (see text).

a bud (for convenience, we also include an empty tree with weight 1). This now results in the relation

$$G_{\mathrm{BMHP}}|_{g^{2n}} = \frac{3}{2(n+2)} S|_{g^{2n}} \tag{6.6}$$

for $n > 0$, with an extra factor of $1/2$ to account for the two choices of bud where to plant the tree.

For g and z non-negative, the good trees generated by S form a family of planted trees with *local non-negative weights* only, characterized by a number of local constraints, and subject to a non-trivial *global* 'goodness' constraint (G3′) that, upon closing, no NHP edge is created. The singularity structure of S is inherited from that of G_{BMHP}, hence the statistics of these good trees undergoes at $z = z_+$ the Ising-like crystallization transition of section 2.3.

As the weights are non-negative, we may rephrase them in terms of probabilities by assigning to each such planted good tree $\mathcal{T}$ with $2n(\mathcal{T})$ vertices and $h(\mathcal{T})$ particles a probability

$$p(\mathcal{T}) = \frac{1}{S} g^{2n(\mathcal{T})} z^{h(\mathcal{T})}. \tag{6.7}$$

By construction, these add up to 1 on the set of planted good trees.

In the case $z = 0$ of maps without particles, the planted trees are generated by $S_0 \equiv S(z = 0)$, solution of $S_0 = 1 + 2g^2 S_0^2$, namely $S_0 = \left(1 - \sqrt{1 - 8g^2}\right)/(4g^2)$, with a singularity at $g^2 = 1/8$. Their probabilities may be associated with those of a branching process as follows. Each tree is interpreted as the genealogical tree of a species whose individuals live at the level of the edges descending from white vertices and are subject to the evolution rules sketched in figure 19. The individuals either die without descendants with probability $(1 - p)$ (if the edge at hand is a leaf) or, with probability p, first make a two-state choice with probability $1/2$ (black vertex with the bud pointing to the left or to the right) and then give rise to two children (the two descending edges of the white descendant vertex of the black one). Comparing with the recursive rules for good trees without particles, this amounts to setting $g^2 = p(1 - p)/2$. This leads to $S_0 = 1/(1 - p)$ if we assume $0 < p < 1/2$, and probability (6.7) of a tree $\mathcal{T}$ reads

$$p(\mathcal{T}) = \left(\tfrac{1}{2}\right)^{n_\bullet(\mathcal{T})} p^{n_\circ(\mathcal{T})} (1 - p)^{n_{\mathrm{leaf}}(\mathcal{T})} \tag{6.8}$$

if the tree has n_{leaf} leaves, $n_\bullet$ black vertices and $n_\circ$ white vertices. This probability matches clearly that of the branching process.

Note that for $p > 1/2$, formula (6.8) still corresponds to the probability of the branching process, but it does not match probability (6.7) for the tree as S_0 is now given by $1/p$. The relative factor $(1 - p)/p$ is nothing but the probability that the branching process remains finite, i.e. that the species become extinct. It is known that this probability is less than 1 for $p > 1/2$. This is a general feature of the so-called Galton–Watson branching processes, with

local evolution rules [32]. These processes undergo a transition at the value of the parameters (here p) at which the average number of children (here equal to $2p$) attains 1. Note that the transition takes place precisely at the singularity of S_0 as $g^2 = 1/8$ when $p = 1/2$. This should not come as a surprise as, when $g^2 \to (1/8)^-$, the average size of the trees diverges, which is the signal that infinite branching processes are about to appear. Note that probabilities (6.7), which add up to 1 by construction, may still be interpreted as those of the branching process provided the latter is *conditioned* to remain finite (i.e. get extinct).

With only probabilistic weights and local evolution rules, branching processes are trapped in the 'universality class' of the Galton–Watson transition. In the tree language, this amounts to always having the same (square-root) singularity structure for generating functions. In the presence of particles, good trees however seem to be a way to escape from this Galton–Watson framework as we know from the above analysis that they undergo an Ising-like crystallization transition at which the singularity has a different nature, namely that of a cubic root responsible for the exponent $7/3$ in equation (2.9). The new ingredient that gives rise to this new universality class is the non-local goodness constraint on the trees. We may again view the good trees and their probabilities (6.7) as describing branching processes with local evolution rules, again conditioned to remain finite, and further conditioned by the (somewhat non-natural) global goodness constraint. A good understanding of this branching process is still lacking. As before, approaching the critical line $g \to g_c(z)$ must correspond to attaining an average number of children equal to 1. It would be interesting to understand:

(i) whether or not the multi-critical point at $z = z_+$ may be attained in the physically acceptable range of parameters;
(ii) if so, what general property of the branching process governs the approach to the multi-critical point.

To this end, it seems likely that a formulation of maps as labelled trees like that described in [20, 33] rather than blossom trees may be more appropriate. Also, a generalization of the goodness condition to infinite trees would be desirable.

On the other hand, the use of the larger class of admissible trees allows us to get rid of the global goodness constraint, but at the expense of having negative weights. Still we might hope to be able to re-interpret these signs as subtractions of overcounted branching processes. In the present blossom tree language however, the trees in the same equivalence classes of a non-admissible map (which add up to zero), have very different shapes and we have not been able to rearrange them to give such a re-interpretation.

7. Conclusion

In this paper, we have shown how to extend the bijective methods of [7–15] to the case of planar bicubic maps with hard particles. In the matrix language, this extends the bijective combinatorial treatment of the one- and two-matrix models to the case of a four-matrix integral with action (1.4) displaying a chain-like interaction. The first lesson to be drawn from this study is that the bijective approach still applies in this case although the matrix model solution clearly indicated the presence of signed weights in the auxiliary counting functions (cf equation (2.2)). We have indeed shown that these signs could be interpreted in terms of a kind of inclusion–exclusion principle, here projecting the generating function of admissible trees onto that of good trees, hence reproducing $G_{\mathrm{BMHP}}(g, z)$. A second lesson is that the cutting procedure of [9], based on paths which are minimal with respect to the canonical geodesic distance on the map, may be extended for each given map to other (less canonical) definitions of the geodesic distance. In particular, the introduction of blocked edges was

instrumental in our proof. Physically, this may be understood as a form of interaction between the space metric (distances on the map) and matter (presence of particles correlated to the blocked edges). This freedom in the choice of the definition of distances may prove useful to tackle other problems, for instance extended hard objects such as hard dimers (occupied edges), animals (occupied clusters), etc.

An interesting property of this study is the robustness of the method, which may be adapted to the case of arbitrary potentials as well as higher order exclusion rules (higher number of matrices). This extends *de facto* the class of problems amenable to a bijective treatment to a much larger family of models. The latter is expected to include all possible (multi-)critical points of two-dimensional statistical models on random surfaces whose universality classes are described by minimal conformal field theories coupled to two-dimensional quantum gravity. All these models may therefore be understood in terms of trees with proper signed weights. In particular, this combinatorial framework provides a unified formulation of both the Ising model and the model of hard particles on bipartite graphs, which eventually explains their common universality class.

Finally, the existence of a tree formulation implies a connection between these map enumeration problems and spatial branching processes. We may hope that these two fields of research may benefit from this connection. In particular, the critical points of maps with generalized particle exclusion rules lying in unitary conformal classes should translate into well-defined branching processes (with positive probability weights). By a global conditioning, we might even be able to escape from the restricted class of Galton–Watson processes and reach in the continuum limit new classes of continuous random trees, generalizing that of [34].

Acknowledgments

All the authors acknowledge the support of the Geocomp project (ACI Masse de données). JB acknowledges financial support from the Dutch Foundation for Fundamental Research on Matter (FOM). PDF acknowledges support from the European network 'Enigma', grant MRTN-CT-2004-5652.

References

[1] Tutte W 1963 A census of planar maps *Can. J. Math.* **15** 249–71
Tutte W 1962 A census of planar triangulations *Can. J. Math.* **14** 21–38
Tutte W 1962 A census of Hamiltonian polygons *Can. J. Math.* **14** 402–17
Tutte W 1962 A census of slicings *Can. J. Math.* **14** 708–22
[2] Brézin E, Itzykson C, Parisi G and Zuber J-B 1978 Planar diagrams *Commun. Math. Phys.* **59** 35–51
[3] Di Francesco P, Ginsparg P and Zinn–Justin J 1995 2D gravity and random matrices *Phys. Rep.* **254** 1–131
[4] Bessis D 1979 A new method in the combinatorics of the topological expansion *Commun. Math. Phys.* **69** 147–63
Bessis D, Itzykson C and Zuber J-B 1980 Quantum field theory techniques in graphical enumeration *Adv. Appl. Math.* **1** 109–57
[5] Ambjørn J, Durhuus B and Jonsson T 1997 Quantum geometry. A statistical field theory approach *Camb. Monogr. Math. Phys.* **1**
[6] Ambjørn J, Chekhov L, Kristjansen C and Makeenko Y 1993 Matrix model calculations beyond the spherical limit *Nucl. Phys.* B **404** 127–72
Ambjørn J, Chekhov L, Kristjansen C and Makeenko Y 1995 *Nucl. Phys.* B **449** 681 (erratum)
[7] Cori R and Vauquelin B 1981 Planar maps are well labeled trees *Can. J. Math.* **33** 1023–42
[8] Arquès D 1986 Les hypercartes planaires sont des arbres très bien étiquetés *Discrete Math.* **58** 11–24
[9] Schaeffer G 1998 Conjugaison d'arbres et cartes combinatoires aléatoires *PhD Thesis* Université Bordeaux I
[10] Schaeffer G 1997 Bijective census and random generation of Eulerian planar maps *Electron J. Comb.* **4** R20

[11] Bousquet-Mélou M and Schaeffer G 2000 Enumeration of planar constellations *Adv. Appl. Math.* **24** 337–68
[12] Bouttier J, Di Francesco P and Guitter E 2002 Counting coloured random triangulations *Nucl. Phys.* B **641**[FS] 519–32 (*Preprint* cond-mat/0206452)
[13] Bouttier J, Di Francesco P and Guitter E 2002 Census of planar maps: from the one-matrix model solution to a combinatorial proof *Nucl. Phys.* B **645**[PM] 477–99 (*Preprint* cond-mat/0207682)
[14] Bousquet-Mélou M and Schaeffer G 2002 The degree distribution in bipartite planar maps: application to the Ising model *Preprint* math.CO/0211070
[15] Bouttier J, Di Francesco P and Guitter E 2003 Combinatorics of hard particles on planar graphs *Nucl. Phys.* B **655**[FS] 313–41 (*Preprint* cond-mat/0211168)
[16] Kawai H, Kawamoto N, Mogami T and Watabiki Y 1993 Transfer matrix formalism for two-dimensional quantum gravity and fractal structures of space-time *Phys. Lett.* B **306** 19–26
[17] Watabiki Y 1995 Construction of noncritical string field theory by transfer matrix formalism in dynamical triangulation *Nucl. Phys.* B **441** 119–66
[18] Ambjørn J and Watabiki Y 1995 Scaling in quantum gravity *Nucl. Phys.* B **445** 129–44
[19] Ambjørn J, Kristjansen C and Watabiki Y 1997 The two-point function of $c = -2$ matter coupled to 2D quantum gravity *Nucl. Phys.* B **504** 555–78
[20] Chassaing P and Schaeffer G 2004 Random planar lattices and integrated superbrownian excursion *Probab. Theory Relat. Fields* **128** 161–212 (*Preprint* math.CO/0205226)
[21] Bouttier J, Di Francesco P and Guitter E 2003 Geodesic distance in planar graphs *Nucl. Phys.* B **663**[FS] 535–67 (*Preprint* cond-mat/0303272)
[22] Bouttier J, Di Francesco P and Guitter E 2003 Random trees between two walls: exact partition function *J. Phys. A: Math. Gen.* **36** 12349–66 (*Preprint* cond-mat/0306602)
[23] Bouttier J, Di Francesco P and Guitter E 2003 Statistics of planar maps viewed from a vertex: a study via labeled trees *Nucl. Phys.* B **675**[FS] 631–60 (*Preprint* cond-mat/0307606)
[24] Chassaing P and Durhuus B 2003 Statistical Hausdorff dimension of labelled trees and quadrangulations *Preprint* math.PR/0311532
[25] See for instance Douglas M 1990 The two-matrix model *Random Surfaces and Quantum Gravity* ed O Alvarez, E Marinari and P Windey (*NATO ASI Series B: Physics* vol 262)
[26] Gaunt D and Fisher M 1965 Hard-sphere lattice gases: I. Plane-square lattice *J. Chem. Phys.* **43** 2840–63
Runnels L, Combs L and Salvant J 1967 Exact finite methods of lattice statistics. II. Honeycomb-lattice gas of hard molecules *J. Chem. Phys.* **47** 4015–20
[27] Baxter R J 1980 Hard hexagons: exact solution *J. Phys. A: Math. Gen.* **13** L61–70
Baxter R J and Tsang S K 1980 Entropy of hard hexagons *J. Phys. A: Math. Gen.* **13** 1023–30
See also Baxter R J 1984 *Exactly Solved Models in Statistical Mechanics* (London: Academic)
[28] Baxter R J, Enting I G and Tsang S K 1980 Hard square lattice gas *J. Stat. Phys.* **22** 465–89
Kamieniarz G and Blöte H 1993 The non-interacting hard-square lattice gas: Ising universality *J. Phys. A: Math. Gen.* **26** 6679–89
[29] Bouttier J, Di Francesco P and Guitter E 2002 Critical and tricritical hard objects on bicolourable random lattices: exact solutions *J. Phys. A: Math. Gen.* **35** 3821–54 (*Preprint* cond-mat/0201213)
[30] Di Francesco P 2002 Geometrically constrained statistical models on fixed and random lattices: from hard squares to meanders *Preprint* cond-mat/0211591
[31] Boulatov D and Kazakov V 1987 The Ising model on a random planar lattice: the structure of the phase transition and the exact critical exponents *Phys. Lett.* B **186** 379–84
[32] Karlin S and Taylor H 1975 *A First Course in Stochastic Processes* (New York: Academic)
[33] Bouttier J, Di Francesco P and Guitter E 2004 Planar maps as labeled mobiles *Electron. J. Comb.* **11** R69 (*Preprint* math.CO/0405099)
[34] Aldous D 1993 Tree-based models for random distribution of mass *J. Stat. Phys.* **73** 625–41